Energy Conversion and Management 154 (2017) 244–261

Contents lists available at ScienceDirect

Energy Conversion and Management

journal homepage: www.elsevier.com/locate/enconman

Techno-economic assessment of different routes for olefins production through the oxidative coupling of methane (OCM): Advances in benchmark technologies

Vincenzo Spallina[a,b], Ildefonso Campos Velarde[a], José Antonio Medrano Jimenez[a], Hamid Reza Godini[c], Fausto Gallucci[a,*], Martin Van Sint Annaland[a]

[a] Chemical Process Intensification, Chemical Engineering and Chemistry Department, Eindhoven University of Technology, Eindhoven, The Netherlands
[b] Group of Membrane Technology, Tecnalia Research and Innovation, San Sebastian, Spain
[c] Process Dynamics and Operations, Technische Universität Berlin, Berlin, Germany

ARTICLE INFO

Keywords:
OCM process
Ethylene production
Energy analysis
Economics
Naphtha steam cracking

ABSTRACT

This paper addresses the techno-economic assessment of two technologies for olefins production from naphtha and natural gas. The first technology is based on conventional naphtha steam cracking for the production of ethylene, propylene and BTX at polymer grade. The unused products are recovered in a boiler to produce electricity for the plant. The plant has been designed to produce 1 MTPY of ethylene.

In the second case, ethylene is produced from natural gas through the oxidative coupling of methane (OCM) in which natural gas is fed to the OCM reactor together with oxygen from a cryogenic air separation unit (ASU). The overall reactions are kinetically controlled and the system is designed to work at about 750–850 °C and close to 10 bar. Since the overall reaction system is exothermic, different layouts for the reactor temperature control are evaluated.

For the naphtha steam cracking plant, the energy analysis shows an overall conversion efficiency of 67% (with a naphtha-to-olefins conversion of 65.7%) due to the production of different products (including electricity), with a carbon conversion rate of 70%. The main equipment costs associated with naphtha steam cracking are represented by the cracker (about 30%), but the cost of ethylene depends almost entirely on the cost associated with the fuel feedstock.

In case of the OCM plant, the overall energy conversion efficiency drops to maximally 30%. In the studied plant design, CO_2 capture from the syngas is also considered (downstream of the OCM reactor) and therefore the final carbon/capture efficiency is above 20%. The cost of ethylene from OCM is higher than with the naphtha steam cracking plant and the CAPEX affects the final cost of ethylene significantly, as well as the large amount of electricity required.

1. Introduction

With more than 140–160 million tonnes per year [1,2], ethylene, the simplest olefin, is by far the most important raw material in the petrochemical industry. Direct applications include, among others, the three polyethylene plastics HDPE, LLDPE, and LDPE as well as petrochemical intermediates, which are in turn mainly used for the production of plastics. Other applications include the production of solvents, cosmetics, pneumatics, paints, packaging, etc. [3].

In Western Europe, liquid naphtha (from crude oil refining) is by far the most important raw material and contributes for 73% in the ethylene production capacity [4]. The cost of olefins follows the cost of feedstock resulting in a considerable cash cost and return for a naphtha cracker plant and therefore in China coal-to-liquids (CTL) and methanol-to-olefins (MTO) [5–7] are becoming economically viable (especially with an oil price above 100 $/bbl). Natural gas processes recover ethane from natural gas through cryogenic separation and then convert it to olefins via an ethane cracking process. Gas as feedstock is less significant in Western Europe mostly because liquid fuels are easy to transport so that it is not essential to co-locate ethylene with a suitable source of feed. Nevertheless, ethylene is also produced from gasoil (10%), butane (6%), ethane (5%), propane (4%) and other sources (2 %). Differently, in the US most of the ethylene plants use light gases cracking, thus reducing the capital costs [8].

* Corresponding author.
E-mail addresses: v.spallina@tue.nl (V. Spallina), f.gallucci@tue.nl (F. Gallucci).

http://dx.doi.org/10.1016/j.enconman.2017.10.061
Received 20 September 2017; Received in revised form 20 October 2017; Accepted 21 October 2017
Available online 05 November 2017

Nomenclature

Acronyms and symbols

ASU	Air Separation Unit
BEC	Bare Erected Cost, M€
BTX	Benzene, Toluene, Xylene
CAPEX	Capital expenditure
CCF	Capital charge factor
COO	Cost of ethylene, €/$t_{C_2H_4}$
HE	Heat exchangers
HP/IP/LP	High/Intermediate/Low pressure
HT/IT/LT	High/Intermediate/Low temperature
MDEA	methyl-diethanolamine
MTPY	Million tons per year
O&M	Operation and Maintenance
OCM	Oxidative Coupling of Methane
OPEX	Operating expenditure
S	Selectivity
TOC	Total Overnight Cost, M€
TSA	Temperature Swing Adsorption
X	Conversion
Y	yield

Subscripts

Chem	chemicals
El	electricity
Feed	feedstock
FTC	Fuel-to-Chemicals
FTE	Fuel-to-Electricity
Th	thermal

Apart from the investment and the cost of the liquid fuel, the naphtha steam cracking process is high energy intensive (about 60% of the energy required in the ethylene production plant is consumed in the cracker [9]) and it is responsible of large CO_2 emissions (estimated between 2 and 3 t_{CO2}/t_{C2H4}) [3,10,11].

In the framework of a fuel switching scenario, natural gas represents an economically more attractive alternative and an environmentally more friendly feedstock due to the cheaper price (in particular in North America with shale gas) while the amount of equivalent CO_2 per energy is about 50% lower than liquid fuels and about 30% lower compared to coal. Natural gas to olefins is possible using two different processes: in the first case (indirect conversion), natural gas is converted into syngas to produce methanol, which is subsequently converted into olefins in a reactor operated at around 500 °C and 2.5 bar. This process can achieve yields in the range between 75% and 90% as in the UOP/Hydro MTO process [5]. A second alternative, and also a more attractive technology, is the direct conversion of CH_4 to C_2H_4 through the oxidative coupling of methane (OCM) [12]. This reaction occurs by feeding CH_4 and O_2 according the reaction equations (1) and (2) producing C_2H_4 and C_2H_6 [12–16].

$$2CH_4 + O_2 \rightarrow C_2H_4 + 2H_2O \quad \Delta H_0^{298K} = -140\ \text{kJ/mol}_{CH_4} \tag{1}$$

$$C_2H_6 + 0.5O_2 \rightarrow C_2H_4 + H_2O \quad \Delta H_0^{298K} = -87.8\ \text{kJ/mol}_{CH_4} \tag{2}$$

Since the 80s, the OCM process has been extensively studied [17]. Several studies have been performed to achieve the optimal catalyst formulation based on metals containing rare-earth oxides [18,19], resulting in some of the most promising catalysts for OCM: Li/MgO [20,21], La_2O_3/CaO [22] and Mn/Na_2WO_4/SiO_2 [23,24]. Mleczko and Baerns [15] proposed a high temperature kinetic model for applications ranging 700 < T < 950 °C and 2.5 < CH_4/O_2 < 10 up to 10 bar in which a set of 10 different reactions were considered. Later, Stansch et al. [16] extended the validity of the kinetic model to a wider range of operating conditions for La_2O_3/CaO deriving the kinetic rate parameters using genetic algorithm optimization methods. Vatani et al. [25] discussed the kinetics of a Li/MgO catalyst extending also the number of reactions to include also the oxidation of ethane to propylene and propane (overall six more reactions) and using a CH_4/O_2 ratio of 2. In their work, they measured CH_4 conversions up to 45% with a C_2 selectivity of 44%. Recently, Liu et al. [26] have scaled up the OCM process using a Mn/Na_2WO_4/SiO_2 catalyst to a volume of 200 ml. In their work, the feed gas was diluted with H_2O and operation was maintained for 100 h reaction time leading to a C_2 selectivity of 61 − 66% and a C_2 yield of 24.2 − 25.4% in a single pass without any significant loss in catalytic performance. Due to the complicated temperature control inside the reactor, Lee et al. [27] have highlighted the risk of hot spot formation and subsequently the decrease in C_2 selectivity (forming CO and CO_2 instead) using different amounts of Mn/Na_2WO_4/SiO_2 (up to 40 g) in the form of pellets. The heat management of the reactor was also discussed by Tiemersma et al. [28–30], who proposed a dual function catalyst to couple the OCM reaction with dry and steam methane reforming. The main issues associated to the reactor design for OCM are the low C_2 yields achieved and the heat management to accomplish the heat removal from the reactor [31–33]. In order to circumvent these drawbacks, the use of membranes (and membrane reactors) has received a lot of attention in recent years [13,28,34–37] showing already higher C_2 yields (up to 35%) by distributive feeding of O_2 along the reactor, which keeps the oxygen partial pressure always low, thus increasing the selectivity towards C_2 instead of CO and CO_2 [38], while also allowing better temperature control.

Up to now, despite the interest in OCM, only few works have been reported in the open literature providing a detailed energy analysis and sizing of large-scale C_2H_4 production plants using OCM. Thiruvenkataswamy et al. [39] have performed a techno-economic and safety analysis and from their analysis it is concluded that the ethane cracking process is more efficient and economically superior while the gas to ethylene process is inherently safer. Godini et al. [34] have performed a techno-economic assessment comparing the classic OCM technology also integrated with dry reforming and an adsorption process in order to reduce the operating costs of CH_4 separation. Overall, it results in 4–5 years of payback time and 90% of CO_2 capture and conversion. Salkuyeh et al. [40] presented a poly-generation process to combine the production of ethylene and electricity with 100% CO_2 capture using chemical looping combustion for the energy recovery in the power generation plant. However, in order to make it advantageous compared with naphtha cracking a cost of CO_2 of 40–45 eur/ton should be considered. However, no details were presented in this work on the benchmark technologies. CO_2 separation from an OCM plant was also discussed in Stünkel et al. [41], who compared a conventional amine absorption process and a hybrid system where CO_2 selective membranes were used to reduce the absorption column size and the duty required for solvent regeneration resulting in a 20% reduction of the energy costs. The present work aims at a detailed techno-economic analysis for similar large-scale plant sizes for different technologies to produce ethylene under the same set of assumptions, which in its turn allows the discussion of the main drawbacks and strengths of the different technologies, as well as guidelines on how to further develop these new strategies towards future industrial deployment.

In the first part of the paper the technical and economic assumptions are presented, as well as a full description of the naphtha steam cracking plant; after that the OCM technology is introduced and the model for the simulation is described. A sensitivity analysis is discussed varying the operating conditions of the OCM unit including also the

heat management strategies, as well as the economic assumptions such as the natural gas and electricity costs.

The OCM configuration is optimized by varying the heat management strategy, syngas dilution, fuel composition, O_2 purity and CH_4/O_2 ratio at the OCM reactor, where the developed OCM model is used for the reactor design and evaluation of its performance.

2. Assumptions and methodology

2.1. Assumptions

The main assumptions used for the calculation of the mass and energy balances are listed in this section. For the main components, the data used for the calculation, the procedure for the sizing and the cost assessment are given. In order to define each component costs, several literature sources have been used as references. Exponential scaling law has been used to calculate the equipment costs as function of scaling parameters as indicated in Table 1. Each cost has later been adapted to the current equipment size and the cost actualized according to the chemical engineering cost index.

(1) Naphtha Cracker: the naphtha conversion is based on literature data [42]. In order to determine the size of the reactor, a residence time of 0.6 s has been considered from which the diameter and length and the total number of coils have been derived.
(2) OCM reactor: the OCM reactor has been modelled according to the kinetic model proposed by Stansch et al. [16] as described in the OCM model (see below), while the cost of the single reactor and internals are derived from the work of Godini et al. [34].
(3) Syngas Coolers: the syngas coolers are modelled as shell and tube heat exchangers in which the minimum pinch temperature difference is assumed equal to 10 °C (liquid-liquid), 10 °C (gas-liquid) and 25 °C (gas-gas) as suggested in the EBTF report [43].
(4) Turbomachines: the blowers, pumps, compressors, expanders and steam turbines are calculated assuming isentropic and electro-mechanical efficiencies from which the thermodynamic conditions of the outlet streams and the energy balance is derived (Table 7).
(5) Distillation columns: the calculation of the distillation columns is based on the RadFrac method using Aspen Plus. In this respect the number of stages, the distillate-to-feed ratio (D/F) and the reflux ratio (RF) are fixed to determine the mass and energy balances of the system. The size of the columns is based on the procedure described by Hassan [44], where the diameter of the distillation columns is calculated according to the maximum superficial velocity based on the gas volumetric flow rate. The maximum velocity is calculated as function of the plate spacing assuming that the maximum column length is never higher than 30 times the diameter of the column. The cost of the column depends on the column weight and the cost of the material chosen.
(6) Air Separation Unit (ASU): the ASU has not been modelled but the mass and energy balances are derived from literature data [45–49]. The specific energy consumption for the production of oxygen with 95% purity is ranging from 200 to 300 kWh_{el}/t_{O2}. In this work the specific consumption has been selected equal to 250 kWh/t_{O2}, corresponding to 0.9 MJ/kg_{O2}. The sizing of the ASU is based on maximum plant capacity available (around 7000 t_{O2}/d per unit).
(7) Acid Gas Removal (AGR): the simulation of acid gas removal is based on aqueous (30%) methyl-diethanolamine (MDEA) solvent. The CO_2 separation efficiency is assumed 100%, while the reboiler heat duty, the electric consumptions of the pump for the solvent circulation, and the specific cost of the complete equipment have been taken from literature [50,51].
(8) Boiler and Furnace: the combustion temperature has been assumed equal to 1100 °C. The amount of air for the combustion has been calculated in order to have 4% of O_2 (%vol.) in the exhaust gas to guarantee a complete combustion of the gases. The maximum steam

Table 1
List of assumptions for the cost calculation of the plant components.

Equipment	Scaling parameter	Ref. Capacity, S_0	Ref. erected cost, C_o (M€)	Scale factor	Ref.
Turbomachines					
Syngas Compressors	Power, MW	39.7	12.14	0.7	[52]
Pumps	Power, MW	197	0.12	0.7	[51]
Air/syngas blower	Power, MW	1	0.23	0.7	[51]
CO_2 compressors	Power, MW	13	9.9	0.7	[51]
Steam turbine	Power, MW	200	33.7	0.7	[51]
Heat exchangers					
Properties					
Syngas coolers, evaporative	1000	$W\,m^{-2}\,K^{-1}$			
Syngas coolers, superheating	50	$W\,m^{-2}\,K^{-1}$			
Syngas coolers, gas-water	200	$W\,m^{-2}\,K^{-1}$			
Gas-Gas heat exchanger	50	$W\,m^{-2}\,K^{-1}$			
Costs					
IT-HT Shell & Tubes	Area, m^2	1000	0.987	0.7	[53]
LT Shell & Tubes	Area, m^2	1000	0.45	0.7	[53]
Condenser	Heat duty, MW_{th}	54.54	0.75	0.66	[52]
Reboiler	Heat duty, MW_{th}	5.7	0.2	0.66	[52]
Cooling tower	Heat duty, MW_{th}	492	14	0.66	[52]
Cryogenic	Heat duty, MW_{th}	32	0.479	0.7	[52]
Boiler	*Heat transfer*	57.2	1.8	0.9	[52]
Distillation columns	*Volume, m^3*	92.3	4.05	0.8	[52]
Refrigeration cycle					[54–56]
Compressors	Power, kW	100	17.87×10^{-3}	0.9	
Condenser	Duty, kW_{th}	1	0.67×10^{-3}	0.9	
Evaporator	Refrigeration duty, kW_{ref}	1	1.698×10^{-3}	0.9	
Other (valve, motor electric, etc.)	10% of tot. eq. cost				
Air separation unit	O_2 flow rate, $kg\,s^{-1}$	28.9	26.6	0.7	[57]
OCM reactor	C_2H_4 production, $10^6 \times t\,y\,s^{-1}$	0.135	11.6	1	[34]
Methanator	Flow rate, m^3/s	6.96	64.6	0.67	[58]

temperature has been taken equal to 500 °C, while the maximum steam pressure is taken as 100 bar as conventionally used in refineries.

2.2. Indexes of performance

Each plant will convert the chemical energy from the fuel feedstock into chemical products (olefins or aromatics), electricity and heat, and will release to the environment part the carbons which are not converted or separated as CO_2. Different indices have been selected to enable a fair comparison of the techno-economic and environmental performance of the studied plants. The plant performance is calculated using two different efficiencies related to the production of olefins (and aromatics) η_{FTC}, and the production/consumption of electricity η_{FTE} (Eqs. (3)–(7)). The carbon conversion (8) accounts for the amount of carbon contained in the feedstock which is converted into chemicals, while the CO_2 emissions ((9)–(11)) account for the direct emissions due to combustion of the gases in the plant and the CO_2 emissions associated with import/export of electricity and heat, assuming that electricity is produced with a natural gas combined cycle (with a net electric efficiency of 58.4%) and that the steam is produced with an industrial boiler from natural gas (with a net thermal efficiency equal to 90% [59,60]). The natural gas combined cycle is based on industrial heavy duty gas turbine (F-class) and HRSG with 3 pressure levels and maximum steam temperature of 565 °C [43].

The total overnight cost (TOC) (see Table 9) computes the specific cost for the production of C_2H_4 using the capital charge rate factor (CCF) which defines a characteristic unit cost of the plant over the life of the plant accounting for all expenditures that occur in different periods on a common value basis. In order to determine the CCF different financial parameters have been used according to [43,61]. On the basis of the financial assumptions (see Table 8), the resulting CCF for the entire plant equals 0.10 (based on Rubin et al. [62]). The operating costs take into account: (i) the cost of the feedstock, and (ii) the credits obtained due to the additional products (such as C_3H_6, BTX) as proposed in Boulamanti, Moya [8], (iii) the variable O & M (as in Table 2) and (iv) the import/export of electricity. The plant availability is assumed equal to 90%.

Overall Energy Balance in the products, MW

$$W_{tot} = \sum W_{chem,i} + \sum W_{EL,in\leftrightarrow out} + \sum W_{TH} \tag{3}$$

Chemical Energy of the i component, MW

$$W_{chem} = \dot{m}_i \times LHV_i \tag{4}$$

With i = C_2H_4, C_3H_6, BTX, oil, H_2, feedstocks

Feedstock-to-Chemicals efficiency, %

$$\eta_{FTC} = \frac{\sum_i W_{chem,i}}{W_{feed}} \tag{5}$$

with i = olefins, aromatics

Feedstock-to-Electricity efficiency, %

$$\eta_{FTE} = \frac{\sum_i W_{EL,IN\leftrightarrow OUT}}{W_{feed}} \tag{6}$$

Overall Energy Efficiency, %

$$\eta_{tot} = \frac{W_{tot}}{W_{feed}} \tag{7}$$

Carbon Conversion, %

$$X_C = \frac{\sum_i \dot{N}_{C_i}}{\dot{N}_{C,feedstock}} \tag{8}$$

with i = olefins, aromatics

CO_2 emissions, kg/s

Table 2
Assumptions for the calculation of the O & M costs [8,51,63]

O & M -Fixed			
Labor costs	M€	1.5 (OCM) 5 (naphtha)	
Maintenance cost	% TOC	2.5	
Insurance	% TOC	2	
Catalyst and sorbent			
OCM catalyst cost	k€/m^3	50	
Lifetime	years	5	
Consumables			
Process water cost	€/m^3	2	
Natural Gas cost	€/GJ$_{LHV}$	2.5	US
		5	EU
		1.2	Saudi Arabia
Naphtha cost	€/t	450	US
		450	EU
		460	Saudi Arabia
Miscellaneous			
Electricity cost	(€/MWh)	35	US
		85	EU
		24	Saudi Arabia
Propylene price	€/t	750	
BTX price	€/t	600	
Heavy oil price	€/t	470	

$$\dot{m}_{CO_2,em} = \sum_i \dot{m}_{CO_2,ex} \pm W_{el}\cdot E_{CO_2,CC} \pm W_{TH}\cdot E_{CO_2,TH}$$

$$E_{CO_2,CC} = 96\frac{g_{CO_2}}{MJ_{el}} \; and \; E_{CO_2,TH} = 63\frac{g_{CO_2}}{MJ_{TH}} \tag{9}$$

Overall O_2 specific emissions, $t_{CO_2}/t_{C_2H_4}$

$$E_{CO_2} = \frac{\sum_i \dot{m}_{CO_2,ex}}{\dot{m}_{C_2H_4}} \tag{10}$$

Cost of Ethylene, $€/t_{C_2H_4}$

$$COO = \frac{(CAPEX_{C_2H_4} + OPEX_{C_2H_4} + C_{O\&M_{fix}})_y}{(\dot{m}_{C_2H_4})_y} \tag{11}$$

CAPEX cost M€/y

$$CAPEX_{C_2H_4} = TOC \times CCF \tag{12}$$

See Table 9 for the calculation of the TOC.

OPEX cost M€/y

$$OPEX_{C_2H_4} = (OPEX_{feedstock} + \sum \pm OPEX_{chem} + OPEX_{el} + OPEX_{O\&M})_y \tag{13}$$

OPEX$_i$[1] M€/y

$$OPEX_i = C_i \times \dot{m}_i \times 3600 \times h_{year} \times 10^{-6} \tag{14}$$

where C_i is the specific cost/price (€/kg), m_i is the flow rate (kg/s) and h_{year} are the number of hours per year.

3. Naphtha steam cracking

3.1. Plant description

Based on the current ethylene market share, naphtha has been selected as feedstock to carry out the techno-economic assessment of the plant as the benchmark technology. The process flow diagram is shown in Fig.1.

For the process simulation of the plant, the selected PiONA (n-paraffins, *iso*-paraffins, olefins–naphthenes and aromatics) analysis of the naphtha composition as reported in Ullmann encyclopedia [42] and

[1] In case of OPEX$_{el}$ the power production is considered (instead of the total flowrate).

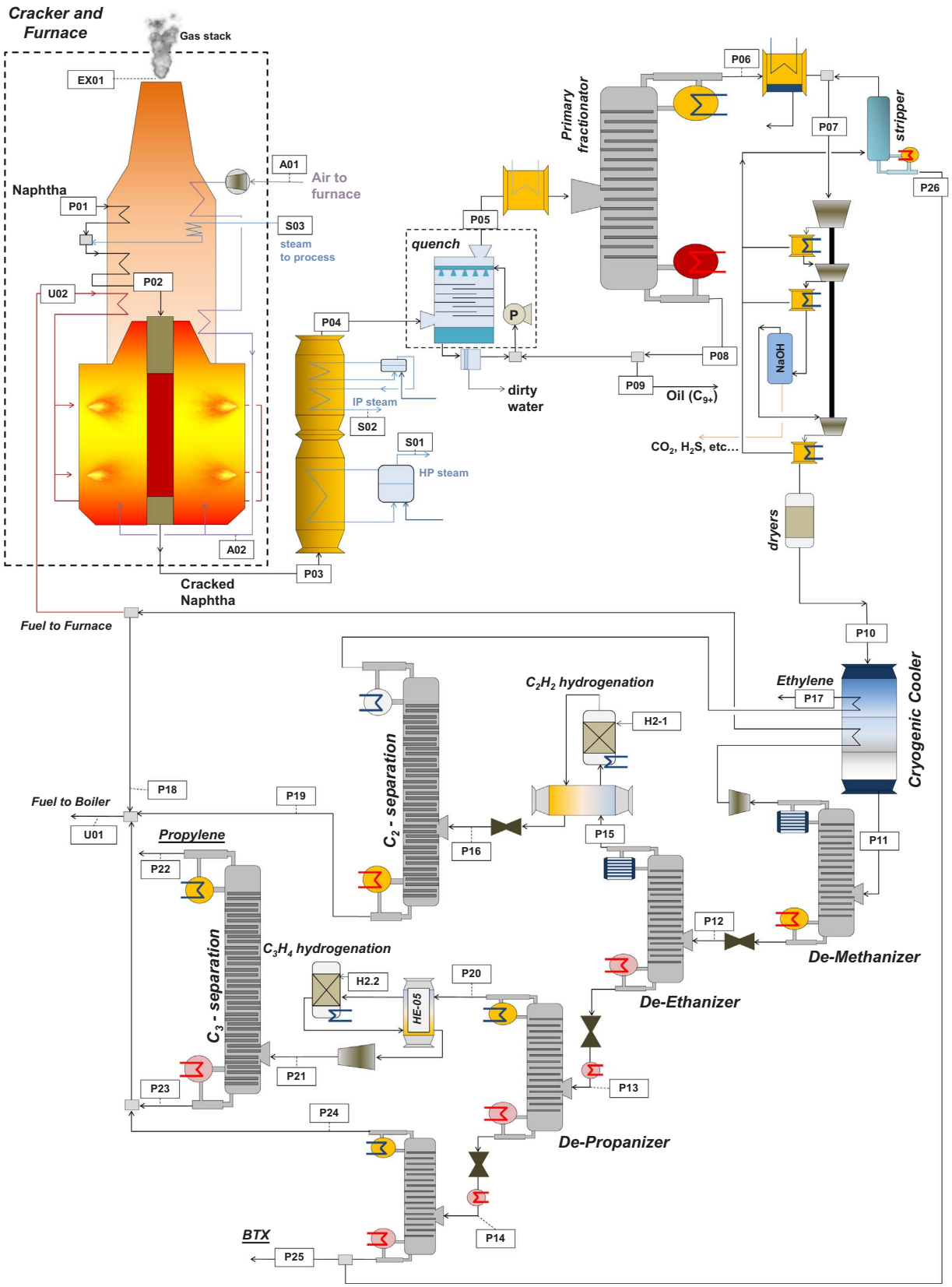

Fig. 1. Flowsheet of the Naphtha Steam Cracking plant. Naphtha conversion and separation units.

the resulting cracked gas are reported in Table 10. Similar results have been achieved also in Haghighi et al. [64].

A naphtha flow rate (stream #P01) equal to 97.22 kg/s (corresponding to 350 t/h and 3.07 MTPY) is pre-heated and mixed with steam (#S03) in order to reach a steam-to naphtha ratio of 0.5 (wt. basis). The mixture is heated-up to 500 °C (#P02) and fed to the naphtha cracker, where a residence time of about 0.6 s has been selected in order to increase the olefins yields operated at 850 °C and

1 bar [42]. According to Zimmermann et al. [42], two furnaces operated in parallel with 200 coils each (with 10.5 cm diameter and 80 m length) are required in order to have the conversion in 0.5 s resulting in an overall volume of 277 m^3. The cracked gas (which is leaving the cracker tubes at 850 °C in #P03) is cooled to 230 °C (#P04) by producing high pressure and intermediate pressure (HP/IP) steam (#S01 and #S02) for power generation. The syngas is then quenched using H_2O and part of the recirculated oil. The resulting gas (#P05) is then cooled down and fed to the primary fractionator where heavy components (C_{9+}) are separated (#P08), while the light components (#P06) are first cooled to ambient temperature and sent to a flash where the gas and liquid streams are separated. The gaseous stream (#P07) is then compressed in an inter-cooled multi-stage compressor up to 31 bar and the liquid knock-out is sent to a stripper for further BTX recovery (P26). During the gas compression (typically in the last stage), the gas is scrubbed with caustic soda (NaOH) to remove acid gas components. The cleaned gas (#P10) is subsequently dried with a molecular sieve and sent to the hydrocarbons fractionating section of the plant. The gas is first cooled down to cryogenic temperature (−50 °C) and fed to the de-methanizer. The incondensable species are released at the top of the columns, expanded to 1 bar and the cooled stream is used to supply part of the refrigeration duty and used as fuel in the furnace (#U02) and in the boiler (#U01). The bottom products are fed at 26 bar (#P12) to the de-ethanizer. The bottom products of the de-ethanizer are subsequently fed in the de-propanizer, and the resulting stream at the bottom is separated in the de-buthanizer. The heavier components are finally sent to the BTX recovery (#P25), while the distillate (#P24) is mixed with the remaining incondensable gasses and used as fuel in the boiler. The distillate of the de-ethanizer is first sent to a hydrogenation reactor, where the acetylene (C_2H_2) is converted into ethylene. Subsequently, the mixture of C_2 species are split in a C_2 splitting column operated at 18 bar with more than 120 stages where ethylene is separated and after the heat recovery is available at polymer grade (#P17). The distillate of the de-propanizer is first sent to an hydrogenation reactor to convert the methyl-acetylene (C_3H_4) to propene (C_3H_6) and secondly sent to a C_3 splitter operated at 21 bar where more than 240 stages are required in order to reach the desired propylene purity (polymer grade) in the distillate stream (#P22). The plant is completely integrated with a steam cycle in which the steam (at different pressures) is produced and distributed around the plant. The heat recovery from the exhaust gas from the furnace is used to pre-heat the reactants at the desired temperature and for steam generation. The steam is generated at 100 bar and superheated up to 500 °C. LP steam is used for the cracking reaction and for the reboilers in the plant. The remaining steam is expanded to 0.08 bar in a turbine (regulated as condensing turbine). The detailed mass balance of the plant can be found in Appendix A.3 (Tables 11 and 12).

3.2. Results and performance

In this process other by-products are produced. In particular, 13 kg/s of propylene, 17.5 kg/s of BTX and 3.8 kg/s of oil are produced, which increases the fuel to chemicals efficiency. In terms of performance, the η_{FTC} is equal to 65.7%. Specifically, the total fuel-to-chemicals is 51% towards C_2H_4 (51%), C_3H_6 (20%), BTX (24%) and heavy oil (6%). The combustion of the incondensable gases is used to produce electricity (gross power 324.9 MW_{el}) to supply the required energy for the auxiliaries of the plant (overall 262.3 MW_{el}). Overall the η_{FTE} equals 1.5%. In terms of electricity consumptions, most of the energy is consumed for the refrigeration cycles used in the cryogenic coolers, and the condenser of the de-methanizer and de-ethanizer (195.07 MW_{el}, 73% of the total auxiliaries consumptions). Most of the remaining consumption is represented by the gas compressor and air fans (overall 22% of the total electricity consumption). The carbon conversion efficiency is 70%, therefore the remaining species are converted to CO_2 (boiler and furnace of the cracker) resulting in overall 2.83 t_{CO2}/t_{C2H4}.

4. Natural gas-to-ethylene

The conversion of natural gas-to-ethylene has been studied through oxidative coupling of methane using different plant layouts, which are explained in the following section.

4.1. OCM reactor model

The kinetic model used for the simulation of the OCM reactor is based on the reaction pathways proposed in the work of Stansch et al. [16], where 10 different reactions have been included (Table 3) and the kinetic parameters have been fitted with experimental results from Liu et al. [26], where 200 ml of 5%wt.Na_2WO_4-1.9wt.%Mn/SiO_2(W-Mn/SiO_2) of 250–600 μm particle was used. The obtained kinetic parameters are reported in Table 4 and it does not depend on the catalyst shape and size. The fitting of the kinetic model has been carried out for five different temperature (in the range of 640–800 °C) for the CH_4

Table 3
List of kinetic expressions for the OCM reaction system [16]

	Reactions	Reaction rate expression
1	$CH_4 + 2O_2 \rightarrow CO_2 + 2H_2O$	$r_j = \frac{k_{0,j} e^{-E_{a,j}/RT} p_C^{mj} p_{O_2}^{nj}}{(1 + K_{j,CO_2} e^{-\Delta H_{ad,CO_2}/RT} p_{CO_2})^2}$
2	$2CH_4 + 0.5O_2 \rightarrow C_2H_6 + H_2O$	$r_2 = \frac{k_{0,j} e^{-E_{a,j}/RT} (K_{0,O_2} e^{-\Delta H_{ad,O_2}/RT} p_{O_2})^{n2} p_{CH_4}^{m2}}{[1 + (K_{0,O_2} e^{-\Delta H_{ad,O_2}/RT} p_{O_2})^{n2} + K_{j,CO_2} e^{-\Delta H_{ad,CO_2}/RT} p_{CO_2}]^2}$
3	$CH_4 + O_2 \rightarrow CO + H_2 + H_2O$	$r_j = \frac{k_{0,j} e^{-E_{a,j}/RT} p_C^{mj} p_{O_2}^{nj}}{(1 + K_{j,CO_2} e^{-\Delta H_{ad,CO_2}/RT} p_{CO_2})^2}$
4	$CO + 0.5O_2 \rightarrow CO_2$	$r_j = \frac{k_{0,j} e^{-E_{a,j}/RT} p_C^{mj} p_{O_2}^{nj}}{(1 + K_{j,CO_2} e^{-\Delta H_{ad,CO_2}/RT} p_{CO_2})^2}$
5	$C_2H_6 + 0.5O_2 \rightarrow C_2H_4 + H_2O$	$r_j = \frac{k_{0,j} e^{-E_{a,j}/RT} p_C^{mj} p_{O_2}^{nj}}{(1 + K_{j,CO_2} e^{-\Delta H_{ad,CO_2}/RT} p_{CO_2})^2}$
6	$C_2H_4 + 2O_2 \rightarrow 2CO + 2H_2O$	$r_j = \frac{k_{0,j} e^{-E_{a,j}/RT} p_C^{mj} p_{O_2}^{nj}}{(1 + K_{j,CO_2} e^{-\Delta H_{ad,CO_2}/RT} p_{CO_2})^2}$
7	$C_2H_6 \rightarrow C_2H_4 + H_2$	$r_7 = k_{0,7} e^{-E_{a,7}/RT} p_{C_2H_6}^{m7}$
8	$C_2H_4 + 2H_2O \rightarrow 2CO + 4H_2$	$r_8 = k_{0,8} e^{-E_{a,8}/RT} p_{C_2H_4}^{m8} p_{H_2O}^{n8}$
9	$CO + H_2O \rightarrow CO_2 + H_2$	$r_9 = k_{0,9} e^{-E_{a,9}/RT} p_{CO}^{m9} p_{H_2O}^{n9}$
10	$CO_2 + H_2 \rightarrow CO + H_2O$	$r_{10} = k_{0,10} e^{-E_{a,10}/RT} p_{CO_2}^{m10} p_{H_2}^{n10}$

Table 4
List of kinetic parameters for the $NaWO_4$-Mn/SiO$_2$ catalyst.

Reactions Units	$k_{0,j}$ mol kg^{-1} s^{-1} Pa$^{-(m+n)}$	$k_{0,j}$[a] mol m$_r^3$ s^{-1} Pa$^{-(m+n)}$	$E_{a,j}$ kJ mol^{-1}	$K_{j,\ CO2}$ Pa^{-1}	$\Delta H_{ad,CO2}$ kJ mol^{-1}	K_{O2} Pa^{-1}	$\Delta H_{ad,O2}$ kJ mol^{-1}	m_j –	n_j –
1	2.00E−03	1.24E−01	80.30	3.50E−13	−172.6			0.64	0.54
2	2.59E+00	1.61E+02	59.15	8.80E−14	−183.2	2.30E−12	−122	1	0.42
3	7.36E−03	4.58E−01	41.18	4.20E−14	−185.1			0.54	0.87
4	1.30E−01	8.09E+00	113.70	4.50E−13	166.3			0.94	0.55
5	9.39E−02	5.85E+00	40.39	5.30E−13	−164			0.92	0.39
6	6.00E+01	3.73E+03	173.70	1.60E−13	−211.5			0.91	0.99
7	1.13E+07[b]	1.13E+07	358.10					0.93	–
8	4.60E+06	2.86E+08	377.70					0.97	–
9	5.81E−01	3.62E+01	142.90					1	1
10	3.98E+00	2.48E+02	145.85					1	1

[a] Assuming 2% active weight content, 60% void fraction.
[b] In this case, the units are: mol m$_r^{-3}$ s^{-1} Pa$^{-(m+n)}$.

conversion (average error 8.9%), C_{2+} and C_2H_4 (average error of 3.3%), CO and CO_2 selectivity (error of 2.8%).

4.2. OCM-based plant description

In this configuration, the natural gas (#P01) is first heated up to 280 °C in order to remove all sulphur compounds in a fixed bed reactor using ZnO. The desulphurized gas (#P02) is then mixed with the unconverted CH_4 and C_2H_6 (and other species), and subsequently fed to the OCM reactor. The O_2 required for the OCM reactions is produced in a cryogenic Air Separation Unit (ASU), where air is first compressed up to 5.26 bar and after drying and CO_2 separation (in a TSA bed) the O_2-N_2-Ar mixture is cooled down to cryogenic temperature and O_2 is separated with 95% purity. Two separation columns are used: the bottom one is operated at high pressure while the one on the top is operated at 1.5 bar and the two columns are thermally integrated since the condenser of the HP columns acts as reboiler of the LP columns. The refrigeration duty of the column is supplied by the cooling effect obtained by two streams from the HP column (respectively, the first rich in N_2 and the second rich in O_2) which are passed through Joule-Thomson valves reducing the pressure and the temperature. The O_2 (with a purity of 95%) is pumped to the OCM pressure and heated up (in which the liquid O_2 is evaporated) supplying part of the refrigeration duty to the cooling of the inlet air to the separation column(s). After that, the N_2 is used to remove the CO_2 from the TSA and vented to the atmosphere (#A02). In case a higher O_2 purity is required, an additional separation column is included to separate Ar-O_2 up to > 99% purity. The ASU modelling is beyond the scope of this work and therefore data from literature were taken from different Refs. [45–49]. In this system, the OCM reactor is considered as a network of different reactors operated in parallel. The reactor configuration is a combination of a cooled packed-bed reactor with additional gas recirculation to dilute the reactants and to avoid hot spot formation inside the reactor (see below). For the base case scenario, a temperature of 850 °C, 10 bar and a CH_4/O_2 ratio equal to 3 have been selected. The internal cooling of the reactor is done by using water evaporation. Due to the very high heat of reaction of the OCM process, this is only possible by using a shell-and-tube configuration [65]. Syngas leaving the reactor is immediately quenched with recirculated cold syngas (#P09) to stop the reaction occurring and the resulting gas (#P04) is sent to syngas coolers, where HP steam at 500 °C is produced for the steam turbine(#W04). Depending on the configuration considered, part of this heat is used to pre-heat the gas used for the dilution inside the OCM reactor. After the complete cooling to ambient temperature, the syngas (#P08) is sent to the CO_2 separation unit with methyl-di-ethanol-amine (MDEA). The CO_2 is compressed and sent for final storage (#P21). The gas from the absorber (#P10) is compressed to 31.5 bar and cooled down to cryogenic temperature (−50 °C). The gas (#P11) is fed to the de-methanizer that operates between −120 and −10 °C. At the bottom of the column the C_2H_4-C_2H_6 rich stream (#P12) is fed to the de-ethanizer, which in its turn works between −32 °C and −15 °C. C_2H_4 with a purity of 99.5% is obtained on the top of the column and after being heated up it is delivered at polymer grade (#P14). The C_2H_6 obtained at the bottom (#P15) is also heated up and subsequently sent to the OCM feed. On the other hand, the top of the de-methanizer is first expanded to the OCM pressure, thus reaching a minimum temperature that is also used to supply part of the duty in the cryogenic cooler. A large part of the CH_4-rich gas (#P17) is sent to the OCM process after a conversion step in which the H_2 and CO present in the stream are fed to a methanator reactor (which operates in a two stage methanator with an intermediate intercooler 400 °C) to increase the CH_4 while a small part is purged and sent to the boiler to avoid inert species accumulation (i.e. N_2, Ar). For the steam cycle, the same operating conditions as in the naphtha steam cracking have been used. The complete mass balance of the plant for the Case #3 is reported in Appendix A.3.

Five different heat management strategies have been considered:

4.2.1. Case #1: Adiabatic OCM

In this configuration, an adiabatic OCM reactor is considered in which the total amount of heat generated is removed by diluting the inlet feed with H_2O or CO_2 (at 350 °C). No external cooling or internal tubes are considered in this configuration.

4.2.2. Case #2: Cooled OCM

In this reactor configuration we assumed to have multiple tubes inside the reactor where HP water is evaporating to produce HP steam for power production. In this case no dilution is considered, but we have assumed a high heat transfer coefficient and heat transfer area from gas to the water to ensure that all the heat produced can be removed from the reactor.

4.2.3. Case #3: Hybrid OCM

In this configuration, a combination of gas dilution (H_2O and CO_2) and internal cooling is considered in the reactor.

4.2.4. Case #4: Dual-stage hybrid OCM

In the fourth scheme, the oxygen feeding to the reactor occurs at two different points in the reactor to perform the OCM reaction with a lower local CH_4/O_2 ratio.

4.2.5. Case #5: Highly selective catalyst

In the last scheme, the kinetics of the catalyst have been varied in order to increase the selectivity toward C_2H_4. In order to perform the simulation of the reactor, the reaction rate of reaction 2 (Table 3) has been increased by a factor 10.

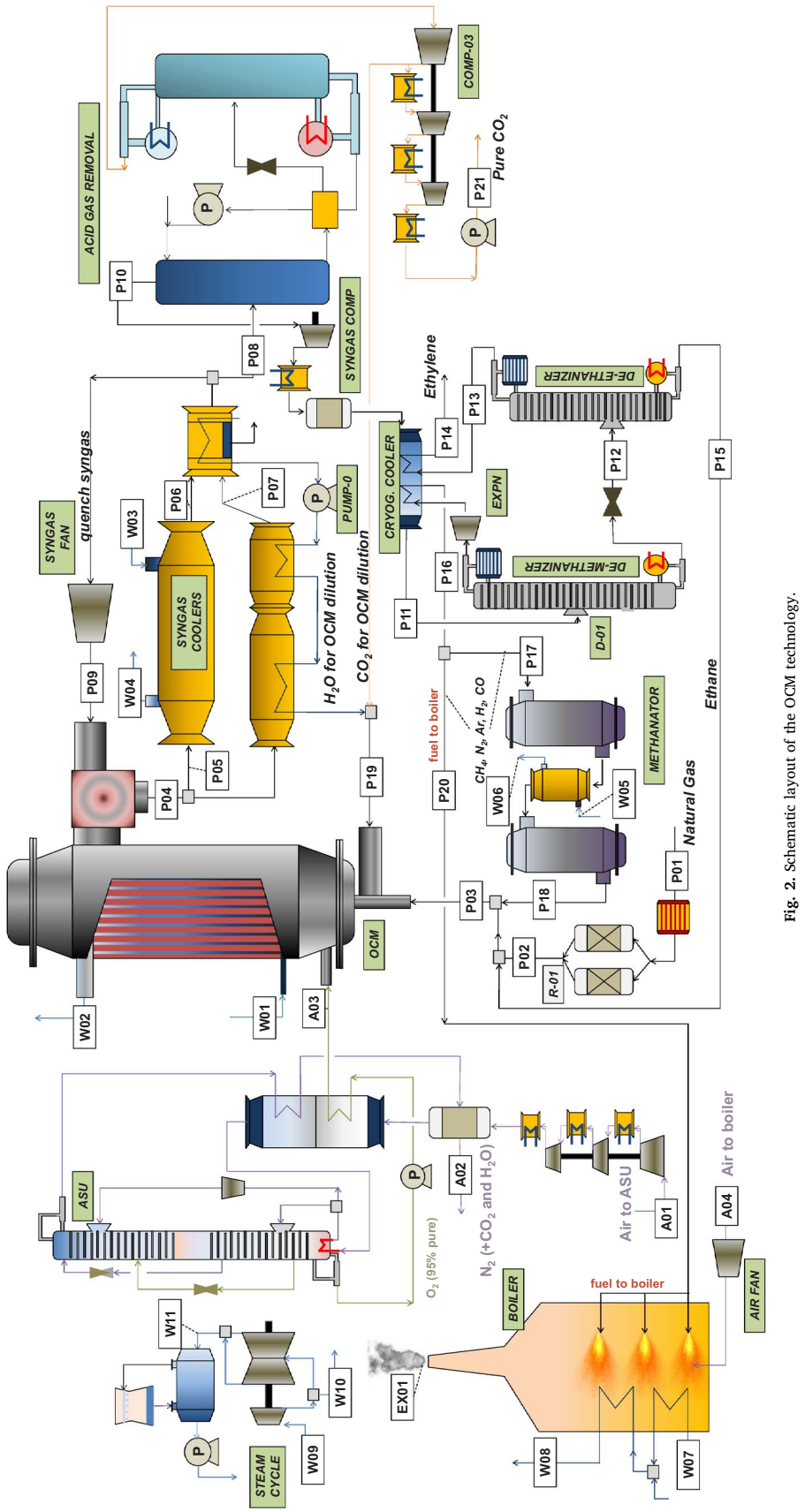

Fig. 2. Schematic layout of the OCM technology.

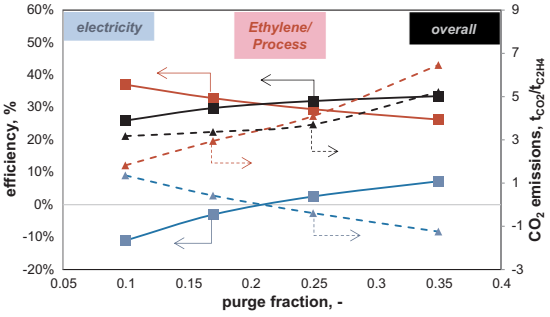

Fig. 3. Sensitivity analysis of Case#2 as a function of the purge fraction.

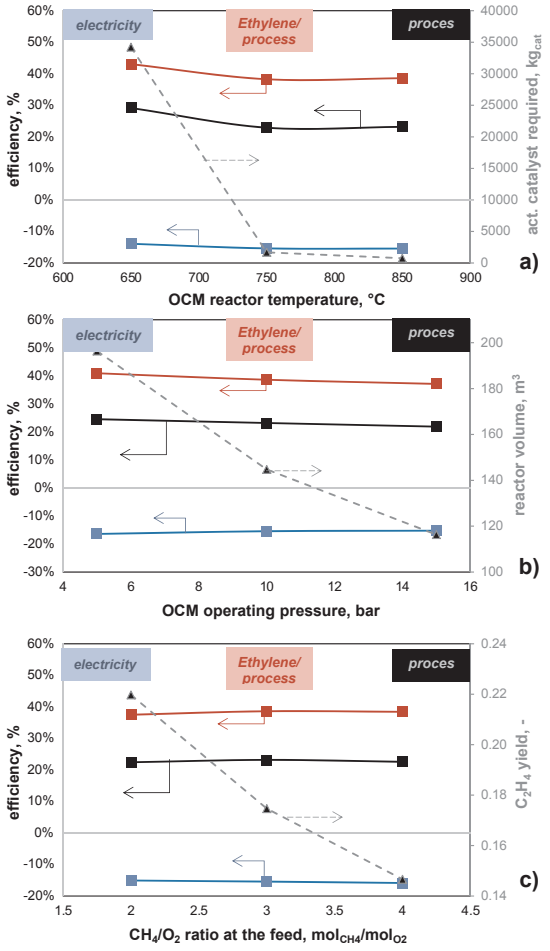

Fig. 4. Results of sensitivity analysis on OCM reactor operating conditions.

5. Results

The results of the techno-economic and environmental analyses will be discussed in two sections: in the first part, the comparison between the OCM plants is discussed, while in the second part, the techno-economic assessment is discussed including also the comparison with the naphtha steam cracking plant. The detailed mass balance of the plant depicted in Fig. 2 for the reference case (case#3) is provided in Appendix A.2 (Table 13).

5.1. Technical comparison

For **Case#1**, the adiabatic OCM, two different configurations have been considered, namely with and without a methanation process. In the case the methanator is not considered in the plant, for a feed ratio CH_4/O_2 equal to 3, the OCM inlet gas contains 40% H_2O. Specifically, about 2.55 kg_{H2O}/kg_{O2} is fed to the OCM reactor. The inlet gas at the OCM reactor also contains 5% CO and 17% H_2 due to the recirculated gas from the de-methanizer (65% of the total flow rate). The ethylene mole fraction y_{C2H4} is 20%, which results from a X_{CH4} of 39.28% and S_{C2H4} of 50.8% for a single pass, while the S_{CO2} and S_{CO} are respectively 31.3% and 31%. The overall energy balance shows a η_{FTC} equal to 25.25% and a η_{FTE} equal to −1.3% for a feedstock flow rate of 129 kg/s of NG (5.95 GW_{LHV}). In this case more than 1.2 GW_{el} are generated by the steam cycle, whereas the energy cost for refrigeration at the condenser of the de-methanizer and the de-ethanizer requires almost 1 GW_{el} (76.1% of the total consumption). This is explained because at the de-methanizer, the bottom/feed weight ratio is 0.11 (0.05 in vol.) and therefore a large cost of cooling is required at the condenser. The ASU and syngas compressor duties represent both in the order of 9–10% of the total auxiliaries, while the CO_2 separation and compression duties are marginal (2.1%). Finally, the cost of H_2O production for the OCM reaction dilution consumes 68% of the total heat available at the gas coolers, thus reducing the amount of steam production for power generation. In case of using a methanator to convert the CH_4-rich recirculation, 3.46 kg_{H2O}/kg_{O2} are required, and the H_2O content is about 60% (vol.). The y_{C2H4} decreases to 19.5% because of a slightly lower S_{C2H4} (49.2%). In this case, the same CH_4/O_2 ratio is used. However, the overall CH_4 and O_2 partial pressures increase inside the reactor (due to a lower dilution by other gases, viz. H_2, CO), which leads to an increase in the η_{FTC} to 28% and a slightly positive η_{FTE} (0.84%) with an overall + 4.9% in the primary energy utilization. The CH_4 content after the methanator shows an increase of 19% and therefore the total amount of natural gas needed in the process is decreased to 116 kg/s (5.35 GW_{LHV}). The cost of refrigeration decreases, mostly because the bottom/feed weight ratio at the de-methanizer is 0.155 (0.08 in vol.). In this case, the cost of H_2O production for OCM dilution increases to 91.5% of the total amount of heat available at the syngas cooling (due to the larger amount of H_2O required), reducing the steam generation. However, some recovery occurs in the intercooling stage of the methanator (2% of the total steam of the steam cycle).

The same adiabatic configuration has been initially considered also using CO_2 instead of H_2O as diluent due to the lower cost of heating. For this case, the dilution required is 4 kg_{CO2}/kg_{O2}, which implies an amount of CO_2 at the inlet of 29.8% (and also a large amount of CO). The resulting η_{FTC} in this configuration decreases significantly to 17.9% compared to the other cases. The y_{C2H4} achieved in this case is just 14.2% because of a X_{CH4} equal to 37.8% and a S_{C2H4} of 37.5%. When giving a closer look at the current kinetic model, it is observed that the amount of CO_2 at the reactor outlet decreases 19.2%, thus resulting in a negative S_{CO2} and in a large production of CO (35% vol. at the reactor outlet). This is explained by the reverse WGS reaction which is close to equilibrium. In fact, the combination of high temperature and low CO/CO_2 molar ratio results in a net CO_2 consumption. In order to implement this configuration, a net amount of pure CO_2 should be produced in the plant and fed at the reactor in order to obtain the required cooling.

In presence of a cooled reactor (**Case#2**), the yield (per single pass) of the OCM reactor decreases from 20% to 18% due to a decrease in both X_{CH4} and S_{C2H4}. This decrease is associated with the higher partial pressures of CH_4 and O_2 in the reactor (the vol. fraction of CH_4 increases to 64.3% and O_2 21.1% compared to the 25.25% and 8.4% of the adiabatic reactor). The η_{FTC} for Case#2 is 26.3% (compared to 28% of Case#1) resulting directly from the low y_{C2H4} of the OCM reactor. However, the η_{FTE} increases to 7.22% (compared to 0.84% of the adiabatic case) because a large amount of electricity is produced (+52%) since no steam-to-process is required for the temperature control in the reactor. In terms of reactor design, the use of cooled reactor would require a lower reactor volume (99.7 m^3 vs. 157.1 m^3) with

Table 5
Energy balance of the C_2H_4 production plants.

Note		NSC	Case#1		Case#2		Case#3		Case#4	Case#5
			No meth.	Methanator	Purge 35%	Purge 10%	Reference	Optimal	2stage O_2 feed	High selective
Feedstock										
Naphtha	kg/s	97.22	0	0	0	0	0	0	0	0
Natural gas	kg/s	0.00	129.02	116	123.88	87.88	85	75.6	73.7	47.5
Thermal input	MW_{LHV}	4274.96	5952.84	5352.11	5715.69	4054.63	3921.81	3488.10	3400.44	2191.60
Chemical products										
Ethylene	kg/s	31.86	31.87	31.82	31.91	31.90	32.17	31.92	31.96	31.98
Purity	%	99.87%	99.54%	99.54%	99.47%	99.42%	99.48%	99.68%	99.56%	99.23%
Propylene	kg/s	13.01	0	0	0	0	0	0	0	0
purity	%	99.43%	0	0	0	0	0	0	0	0
BTX	kg/s	17.48	0	0	0	0	0	0	0	0
Other	kg/s	3.78	0	0	0	0	0	0	0	0
Fuel-to-chemicals	%, $_{LHV}$	65.7%	25.25%	28.04%	26.32%	37.10%	38.69%	43.15%	44.32%	68.82%
Carbon conversion	%	70.1%	30.12%	33.45%	31.41%	44.26%	46.15%	51.48%	52.88%	82.10%
Electricity										
Steam cycle	MW	321.12	1226.13	939.5	1428.26	844.11	557.49	475.98	441.21	**124.1**
Expander	MW	2.97	17.23	9.96	10.09	12.45	12.18	9.97	9.45	3.32
Gas compressor	MW	−38.92	−124.24	−77.01	−82.82	−106.73	−98.19	−81.19	−77.52	−33.79
Refrigeration cycle	MW	−195.07	−991.47	−626.28	−740.90	−1005.08	−885.54	−731.51	−699.1	−309.15
O_2 production	MW	0.00	−115.54	−118.22	−128.32	−139.8	−133.47	−112.3	−107.87	−47.27
CO_2 sep. & cond.	MW	0.00	−27.74	−30.19	−20.35	−29.57	−32.16	−25.7	−24.21	−5.31
Air fans	MW	−20.71	−37.75	−29.96	−32.75	−10.37	−9.62	−7.85	−7.47	−2.48
Heat rejection	MW	−7.22	−23.78	−22.69	−20.76	−13.89	−15.5	−12.33	−12.21	−4.34
Net electricity	MW	62.17	−77.16	45.11	412.46	−448.88	−604.81	−484.93	−477.72	−274.92
Fuel-to-electricity	%, $_{LHV}$	1.5%	−1.3%	0.8%	7.2%	−11.1%	−15.4%	−13.9%	−14.0%	−12.5%
Overall energy	%, $_{LHV}$	67.2%	24.0%	28.9%	33.5%	26.0%	23.3%	29.3%	30.3%	56.3%
Olefins production										
Operating temperature	°C	850	850	850	850	850	850	650	850	**850**
Operating pressure	bar	1	10	10	10	10	10	10	10	10
CH_4-to-O_2 ratio	mol. basis	0	3	3	3	3	3	3	3	3
$X_{CH4,ss}$, conversion		0	0.39	0.40	0.39	0.39	0.40	0.41	0.42	0.54
y_{C2H4} yield		0.33	0.20	0.20	0.2	0.165	0.175	0.206	0.215	0.488
Reactor volume	m3	–	157.10	157.1	126.7	117.8	157.1	603.2	137.4	98.2
C_2H_4 @separation	%vol.	39.5%	4.6%	7.3%	4.7%	5.3%	5.8%	7.0%	7.3%	16.03%
H_2O-to-fuel ratio	kg/kg	0.50	1.03	1.83	0.00	0.00	0.79	0.75	0.75	0.64
CO_2 emissions										
Direct CO_2 emissions	t_{CO2}/t_{C2H4}	2.83	5.27	6.46	4.05	1.82	1.36	1.10	1.05	0.32
CO_2-from-electricity	t_{CO2}/t_{C2H4}	−0.19	0.23	−0.14	−1.24	1.35	1.80	1.46	1.44	0.83
Total CO_2 emissions	t_{CO2}/t_{C2H4}	2.64	5.51	6.33	2.81	3.17	3.16	2.56	2.49	1.15
CO_2 capture rate	%	0.0%	19.3%	23.4%	8.3%	30.3%	34.0%	30.6%	29.5%	45.8%

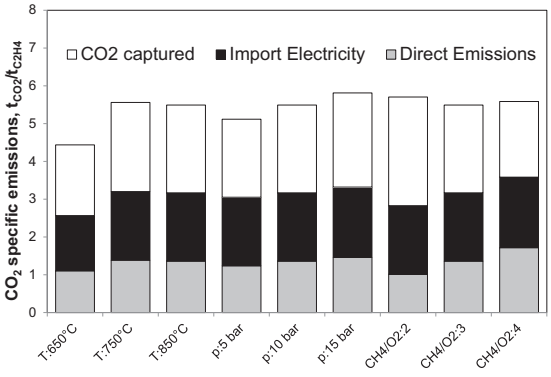

Fig. 5. Carbon conversion and CO_2 emissions for Case#3.

a heat transfer surface area[2] per unit volume of 11 m^2_{HE}/m^3_r. In order to increase the η_{FTC}, a large fraction of the gas can be recirculated to the OCM reactor instead of using it in the boiler. This also implies that the purge fraction has to be decreased down to 0.1 (from 0.35), and the results of this analysis are presented in Fig. 3. By reducing the purge fraction, the η_{FTC} increases up to 37% because more CH_4 is recirculated to the reactor. However, this positive effects bring along a decrease in the η_{FTE} (−11%) because less fuel is used in the boiler (−40%) and all the electric consumptions increase. In particular, more O_2 is required from the ASU (+9%) and the refrigeration unit and syngas compressors consumptions (respectively +36% and +29%) increase due to the higher gas flow rate sent to the cryogenic distillation units. Overall, the energy efficiency decreases from 33.5% to 25.9%. Increasing the recirculation fraction to the reactor reduces the y_{C2H4} (from 18% to 16.5%) mostly because the S_{C2H4} drops from 46.3% to 42.1%. From an environmental point of view, the CO_2 specific emissions decrease at lower purge fraction: on the one hand, the lower electricity consumptions (and eventually net electricity production for a purge factor > 0.2) reduce the CO_2 emissions associated with the auxiliary consumptions. On the other hand, a large η_{FTC} increases the carbon conversion from 15.7% to 22.1% and increases also the amount of CO_2 captured from 14.8% to 30.2%.

In order to maximize the η_{FTC}, a different analysis has been carried out for **Case#3** in which the purge fraction is kept at 10% and the cooling of the reactor is carried out partly with H_2O/CO_2 recirculation (Case#1) and direct cooling (Case#2). The pure O_2-to-dilutant ratio has

[2] The heat transfer area has been calculated assuming a constant global heat transfer coefficient U = 1000 W/m^2 K, constant temperature at the hot side (the reaction temperature) and constant temperature in the cold side $T = T_{sat,H2O}(100\ bar) \approx 350$ °C.

Table 6
Detailed comparison of the economics of the selected plants (in Europe).

		Case#1	Case#1 + meth	Case#2	Case#3ref	Case#3opt	Case#4	Case#5	Naphtha
Turbomachines + steam cycle	% of BEC	34.5%	28.3%	20.6%	17.5%	17.5%	17.4%	10.6%	34.2%
Reactors		8.0%	25.3%	24.7%	25.6%	27.3%	27.3%	30.1%	29.5%
HE + cond + rebs		2.2%	2.2%	2.2%	2.6%	2.1%	2.6%	2.1%	8.4%
Refrigeration units		37.8%	25.7%	35.1%	34.7%	33.5%	33.1%	45.2%	21.4%
Distillation columns		2.0%	2.0%	1.8%	2.0%	2.3%	2.4%	1.9%	6.5%
Air Separation Unit		7.0%	7.4%	7.4%	7.9%	8.0%	8.0%	6.2%	
CO_2 separation		8.5%	9.1%	8.2%	9.7%	9.3%	9.1%	4.0%	
BEC	M€	1073.86	1043.20	1168.95	1055.25	922.05	895.87	654.45	409.88
TOC	M€	2534.09	2461.75	2758.50	2490.17	2175.85	2114.08	1544.38	967.24
Specific cost	M€/(ton/h_{C2H4})	9.35	9.08	10.18	9.19	8.03	7.80	5.70	3.57
				Operating costs					
Feedstock	€/ton_{C2H4}	931.96	840.96	635.61	612.94	546.44	532.04	342.60	1373.16
Electricity/by-products		57.06	−33.49	332.43	446.36	357.25	352.97	184.18	−723.09
O & M		127.75	128.48	139.02	125.44	110.87	109.86	109.76	77.64
Cost of C_2H_4	€/ton_{C2H4}	1396.32	1208.52	1411.76	1458.89	1254.75	1234.76	876.22	834.68

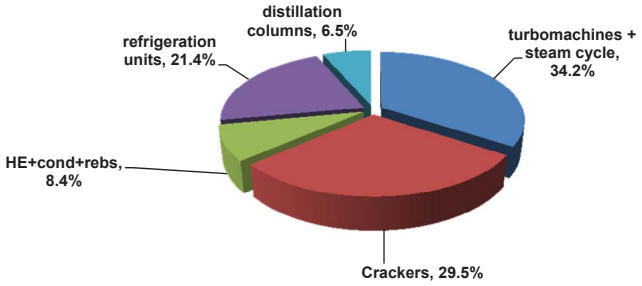

Fig. 6. Bare Erected Cost (BEC) for the Naphtha Steam Cracking plant, percentage of the total BEC.

been fixed equal to 2 $kg_{O2}/kg_{(CO2+H2O)}$. In case only H_2O is used, the y_{C2H4} is 16.2%. The amount of heat removed by the internal cooling deceases to 9.8 MJ_{th}/kg_{C2H4} with respect to 17.6 MJ_{th}/kg_{C2H4} of the equivalent Case#2. The total reactor volume is 133 m^3 which is respectively 12% higher than Case#2 (cooled) and 18% smaller than Case#1 (adiabatic). The η_{FTC} is 38.6% (+1.6% with respect to Case#2), while the η_{FTE} decreases to −15.4%.

Two other cases have been investigated adding CO_2 (respectively 20% and 40% on wt. basis) to the total mass flow rate of diluent to investigate its effect on the performance. While increasing the amount of CO_2, the amount of heat to be removed decreases to 7.8 MJ_{th}/kg_{C2H4}. This results from the combination of a higher gas flow rate and the higher heat capacity of CO_2 compared with H_2O. While increasing the amount of CO_2 the overall volumetric flow rate decreases due to the different molecular weight of CO_2/H_2O ($MW_{CO2} > MW_{H2O}$) as well as the CH_4 and O_2 partial pressures, decreasing slightly the y_{C2H4} (from 16.2% to 15.7%), which reduces consequently the η_{FTC} from 38.6% to 35.8%. In terms of energy performance, also the η_{FTE} decreases at high CO_2 fraction as a consequence of two different effects. On the one hand, the gross electricity production of the steam cycle increases due to a lower amount of heat required for the production of steam for the process. On the other hand, the LP steam required at the reboiler of the AGR units increases (from 73.8 MW_{th} to 195.6 MW_{th}) due to the higher CO_2 amount to be removed (the CO_2 mol. fraction increases from 7.7% to 16.5%), the cost of the refrigeration for the de-methanizer increases due to a larger dilution of C_2H_4 which decreases from 5.8% to 5% at the inlet of the cryogenic units (lower yield) and, finally the cost of CO_2 recompression increases significantly (+40.4 MW_{el}).

The relevant effect of the OCM performance on the overall plant performance suggests a sensitivity analysis on the operating conditions of the OCM. The results of the sensitivity analysis are summarized in Fig. 4a–c and the following trends are highlighted:

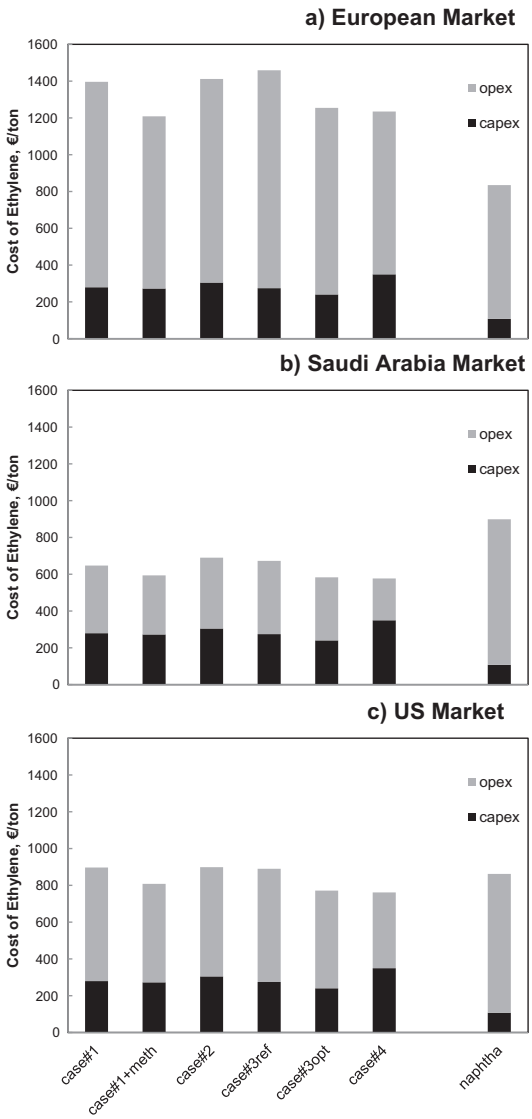

Fig. 7. Economic comparison of different OCM technologies and naphtha steam cracking with three different scenarios.

- A decrease in the OCM temperature from 850 °C to 650 °C shows an increase (+4%) in the η_{FTC} as consequence of an increase in the selectivity towards C_2H_4 from 0.44 to 0.5. Moreover, the η_{FTE}

slightly decreases (−1%) since the cost of refrigeration at the de-methanizer decreases as the concentration of C_2H_4 at the inlet of the cryogenic unit increases up to 6.97% (with respect to 5.8%). Furthermore, it implies that the gross power production from the steam cycle decreases, since more fuel is converted to ethylene. In case of the LT OCM system, the amount of steam produced in the syngas cooler decreases significantly, since less gas is used to quench (from 142 to 31 kg/s), while the overall heat to be removed in the OCM through the HP steam production increases significantly[3] (2.7 times higher). As shown in Fig. 4a, the lower temperature affects significantly the kinetics and therefore both an increase of the active weight content of the catalyst and an increase in the reactor volume are required to reach full conversion of the O_2 along the reactor (more than 44 times). However, Case#3 at 650 °C represents the optimal configuration in terms of performance compared to the other configurations.

- As previously described, a lower O_2 partial pressure increases the S_{C2H4}. Therefore, by increasing the OCM operating pressure from 5 to 15 bar, the y_{C2H4} decreases (from 0.19 at 5 bar to 0.16 at 15 bar) and consequently also the η_{FTC} decreases from 41% to 37%. On the other hand, the η_{FTE} decreases (−1.2%) at lower pressures mostly because of the higher costs of syngas compression (2.1 times higher) to the distillation units. In terms of OCM reactor design, the lower pressure decreases the gas density inside the reactor. Therefore, in order to limit the superficial gas velocity, the reactor volume increases up to 70% (relative to the case at 15 bar) as represented Fig. 4. Moreover, the lower pressure also shows an impact on the volume of the heat exchangers and CO_2 separation columns, as well as in the cost of the syngas compressors.
- By varying the CH_4/O_2 ratio from 2 to 4, a decrease in the X_{CH4} from 58% to 30% and an increase in the S_{C2H4} from 38% to 48% is measured, which overall results in a decrease in the y_{C2H4} (Fig. 4c). The η_{FTC} trend is not constant: this is associated with the fact that at higher CH_4/O_2 ratios the amount of CH_4 that is recirculated increases, thus decreasing the overall feedstock. In terms of energy consumptions several effects can be highlighted: (i) the gross production from the steam turbine remains more or less constant (557–573 MW depending on the case) because by increasing the CH_4/O_2 ratio, more heat is available at the syngas coolers to produce HP steam for power generation (less H_2O is produced for the dilution), and low amount of heat of reaction in the OCM reactor is released; (ii) the consumptions of the ASU increases at the lower CH_4/O_2 ratio, (from 117 MW to 158 MW); (iii) the consumption of the cryogenic cycles increases (+50 MW) at a high CH_4/O_2 ratio due to the high CH_4 content to be separated. It must be noted that in case of a CH_4/O_2 ratio equal to 4 the amount of heat to be removed in the OCM reactor is 1.76 MJ_{th}/kg_{C2H4} (while in case of a CH_4/O_2 ratio equal to 2 this value amounts 15.9 MJ_{th}/kg_{C2H4}) making the heat management of the reactor simpler and easier to be controlled.

The CO_2 emissions are resulting from the combustion of the purge gases (1.1–1.7 t_{CO2}/t_{C2H4}) and from the equivalent CO_2 emissions produced due to the relatively large electricity import (1.46–1.87 t_{CO2}/t_{C2H4}). The CO_2 capture rate of the total CO_2 produced in the plant (including the electricity imported) is ranging between 35.8% and 50.8% (in case of a CH_4/O_2 ratio equal to 2) and it is proportional to the CO_2 selectivity of the OCM reaction system.

In **Case#4** the OCM reactor is arranged as two units in series so that two different feeding points are considered. The CH_4/O_2 ratio is locally always lower than 6, which leads to an increase in the final S_{C2H4} up to 51.6% and a X_{CH4} of 41.7% with a final y_{C2H4} equal to 0.215. The performance of the plant increases significantly; the η_{FTC} increases to 44.2% and also the power consumption decreases (overall η_{FTE} equal to −14.1%). The energy cost of the de-methanizer is reduced due to the high C_2H_4 content (7.3%). The overall CO_2 emissions are 2.49 t_{CO2}/t_{C2H4} (57.6% resulting from the import of electricity) and the carbon capture rate is 41.4% (1.75 $t_{CO2,capt}/t_{C2H4}$). The detailed energy balance of the described plants are summarized in Table 5.

In **Case#5,** the improved kinetics increases the CH_4 conversion (up to 54%) and the C_2H_4 yield goes to 48.8%. A larger amount of C_2H_6 is also produced at the OCM reactor outlet (> 5%, compared to < 0.4% for the other cases) and the reduction of the cost of refrigeration is remarkable (about 30% of the corresponding Case#3) due to the higher amount of C_2H_4 at the separation train (16% respect to about 5% of the other cases) (see Fig. 5).

5.2. Cost assessment

The results of the economic analysis are presented in Table 6. The BEC has been listed for the main group of components. For the conventional naphtha steam cracker, the largest cost is associated with the cracker (except for the combined turbomachines and steam cycle). The bare erected cost (BEC) is 409.9 M€. The costs of the different equipment are shown in Fig. 6. The CAPEX impact to the final cost of ethylene is about 13% (as from Eqs. (11) and (12)).

On the basis of the financial model, the resulting cost of C_2H_4 is 861.8 €/ton, which is higher than the cost predicted in Boalamenti et al. [8] mostly due to the different way used to account for the credits. The cost of the feedstock results in 1373.2 €/ton_{C2H4}. However, the presence of multiple products (C_3H_6, BTX) as well as the electricity production reduces the cost of ethylene production.

In the case of OCM plants, the refrigeration units also represent the highest part of the CAPEX (21.4–35.1% of BEC), which is related to the high energy requirements of the compressors to obtain the required cooling. An improvement in the C_2H_4 yield as well as a more convenient CH_4 separation technique would enhance also the economics of the OCM technology. The cost of the OCM reactor just accounts for about 9% of the total BEC, while the cost of the methanator is about twice higher. This is related to the large volumetric CH_4 flow rate (almost 50%) in the recirculating gas in which the H_2 and CO are converted into CH_4. It should be noted that in this work the option to separate CH_4 from the H_2 and CO has not been considered in order to avoid additional costs of refrigeration (the temperature for a CH_4/CO separation is about −160 °C). The cost of the power plant and the turbomachines is higher when a large purge fraction is considered. It must be noticed that the ASU and the CO_2 separation system account for 8% and 9% respectively. The overall specific cost of the plant is between 7.8 and 10.2 €/(ton_{C2H4}/h), which is more than double in comparison to the specific investment cost for the naphtha steam cracking (3.57 €/(ton_{C2H4}/h)). The costs of the feedstock accounts for 45% (except for Case#1) of the total cost of ethylene, while the large electricity import required represents more than 24% of the total costs (except for Case#1). Finally, in case of a more reactive and selective catalyst (Case#5), and thus improved C_2H_4 yield, the cost of C_2H_4 becomes competitive with the cost of C_2H_4 using naphtha also in the European market.

Based on these results, a sensitivity analysis has been carried out by varying the operating costs (feedstocks and utilities) based on three different markets, specifically in Europe (the reference scenario in Fig. 7a), Saudi Arabia and the United States. This analysis is required mainly due to the uncertainties associated with the cost of the feedstock (both naphtha and natural gas price are affected by several geo-political events). In case of Saudi Arabia (Fig. 7b), the low price of the natural gas (1.2 vs 5 €/GJ of EU) and the electricity, the results are very advantageous for ethylene production through the OCM technology compared to the naphtha steam cracking process. This is partly confirmed by the fact that most of the C_2H_4 production (about 88%) in

[3] The heat of reaction in the OCM reactor depends on CH_4/O_2 ratio and it is removed as sensible heat of the products, which depends on final temperature and flow rate, and heat used to evaporate HP steam.

Saudi Arabia is carried out using ethane and propane as feedstock. In the case of the United States (Fig. 7c) the cost of C_2H_4 using OCM and naphtha is comparable (and therefore in the range of error which is typically ± 30% for the economic analysis). The results of the economic analysis demonstrate that in the presence of a large availability of natural gas at low price, the OCM technology can be competitive with the conventional naphtha steam cracker. However, the current technology readiness level and the high capital cost associated with the OCM plant hinder at the moment commercialization and deployment by chemical companies, especially for large-scale C_2H_4 plants.

6. Conclusions

Two plants based on naphtha steam cracking and oxidative coupling of methane for the production of ethylene have been studied and compared in this work from a techno-economic point of view. The naphtha steam cracking has shown better performances over the OCM technology due to the higher yields and reduced electricity consumptions. In order to improve the fuel-to-olefins efficiencies in the OCM system, lower pressures and lower temperatures are beneficial. In the OCM plants the cost of refrigeration, in particular in the de-methanizer, is by far the most relevant energy cost due to the low concentration of C_2 components and high amount of unconverted CH_4 in the OCM reactor. The techno-economic analyses have shown that lower selectivity increases significantly the cost of C_2H_4 production, mostly because of high electricity import. At a lower temperature (650 °C) or in the presence of a distributive feeding of oxygen (as for the two-stage OCM), the cost of C_2H_4 decreases by 15%. In terms of economics, the classic OCM technologies are not competitive due to the large thermal input and high electricity consumption. In case of a relatively high natural gas price scenario (as in the western European market), the OCM technology becomes competitive with the more established naphtha steam cracking only in case the C_2H_4 yield is about 50%, which allows reaching a fuel-to-chemicals efficiency above 65% (as for the naphtha steam cracking), due to the reduction in the feedstock use and secondarily due to the reduced cost of electricity import. At medium and low natural gas price as in the case of Saudi Arabia and partly in the US, the OCM technologies may become more competitive and even more advantageous than the conventional naphtha steam cracking, although the ethane cracking technologies is the most preferred and used technology for C_2H_4 production in these regions.

However, nowadays the high investment costs for the OCM technologies, the large difficulties to demonstrate the technology at large scale and the uncertainty in the performance of the OCM reactor and its long term stability limit its viability at industrial scale and further demonstration studies are required. Also, the expected higher capital cost associated with the OCM plants represents a strong limitation for the implementation of OCM technology, despite the fact that the resulting cost of ethylene may become competitive with that of the conventional naphtha steam cracking process. On the basis of these results, the impact of integrating membrane and membrane reactor with OCM reactor will be studied in a future work to assess the performance of the plant in presence of higher C_2H_4 yield and cheaper air separation cost.

Acknowledgements

The authors are grateful to the European Union's HORIZON2020 Program (H2020/2014-2020) for the financial support through the H2020 MEMERE project under the grant agreement n° 679933.

Appendix A

A.1. Assumptions

Tables 7–9

Table 7
Main parameters used for the modelling of turbomachines.

Components	η_{is}	η_{m-e}	Cost reference
Blowers	0.75	0.95	[63]
Compressors	0.85	0.95	[53,66]
Pumps	0.85	0.95	[53,66]
Expander	0.85	0.99	[53,66]
HP steam turbine	0.85	0.99	[50]
LP steam turbine	0.75	0.99	[50]

Table 8
Assumptions for the financial model.

Financial model	
Inflation	0.03
Taxation rate	0.35
Depreciation (Year)	20
Debt interest rate	0.05
Revenue interest rate	0.15
Revenue fraction	0.4
Debt fraction	0.6
Construction Payment Years	3
→payment 1st year	40%
→payment 2nd year	30%
→payment 3rd year	30%
Life time	25
Equivalent hrs	7884
Construction years	3

Table 9
Methodology for the calculation of the TOC from NETL [67,51]

Plant component	Cost (M€)
Component W	A
Component X	B
Component Y	C
Component Z	D
Bare erected cost [BEC]	A + B+C + D
Direct costs as percentage of BEC	
Includes piping/valves, civil works, instrumentation, steel structure, erections, etc.	
Total Installation Cost [TIC]	80% BEC
Total Direct Plant Cost [TDPC]	BEC + TIC
Indirect costs [IC]	14% TDPC
Engineering procurement and construction [EPC]	TDCP + IC
Contingencies and owner's costs (C & OC)	
Contingency	10% EPC
Owner's cost	5% EPC
Total contingencies & OC [C & OC]	15% EPC
Total Overnight Cost [TOC]	EPC + C & OC

A.2. Naphtha steam cracking validation

Table 10

Table 10
Naphtha composition selected for the plant analysis and comparison of the cracked syngas with Ullmann [42].

Species		H_2	CH_4	C_2H_4	C_3H_6	C_3H_8	C_4H_{10}	C_5H_{12}	C_6H_{14}	C_7H_{16}	C_8H_{18}	C_9H_{20}
Naphtha composition	wt%, dry					*0.010*	*0.038*	*0.089*	*0.213*	*0.125*	*0.123*	*0.035*
Syngas	wt%, dry	0.004	0.163	0.324	0.145	0.003	0.001		0.001			0.003
Syngas [42]	wt%, dry	0.009	0.169	0.303	0.136	0.004	0.002					
Deviation	%	50%	3%	−7%	−7%	19%	12%					
Species		$C_{10}H_{22}$	$C_{11}H_{24}$	C_5H_{10}	C_6H_{12}	C_7H_{14}	C_8H_{16}	C_9H_{18}	$C_{10}H_{20}$	$C_{11}H_{22}$	C_6H_6	C_7H_8
Naphtha composition	*wt%, dry*	*0.025*	*0.070*	*0.050*	*0.061*	*0.050*	*0.020*	*0.015*	*0.010*	*0.005*	*0.037*	*0.018*
Syngas	wt%, dry										0.096	0.034
Syngas [42]	wt%, dry										0.083	0.034
Deviation,%											−15%	−1%
Species		C_8H_{10}-EB	C_8H_{10}-X	C_8H_8	C_2H_2	C_2H_6	C_3H_4-MA	$C_4H_{4=}$	$C_4H_{6=}$	$C_4H_{8=}$	$C_{12}H_{26}$	C_9H_{12}
Naphtha composition	*wt%, dry*	*0.001*	*0.003*	*500 PPM*								
Syngas	wt%, dry	0.007	0.015	0.012	0.012	0.030	0.015	0.003	0.054	0.033	0.033	0.009
Syngas [42]	wt%, dry	0.004	0.011	0.014							0.052	
Deviation,%		−70%	−32%	17%							19%	

A.3. Naphtha steam cracking mass balance (refer to Fig. 1)

Tables 11 and 12

Table 11
Mass balance of the naphtha steam cracking plant shown in Fig. 1 – part A.

#stream	T	p	LHV	Flowrate				Composition, mol.												
	°C	bar	MJ/kg	kmol/s	kg/s	MTPY	m^3/s	H_2	H_2O	N_2	O_2	CO	CO_2	CH_4	C_2H_4	C_3H_6	C_3H_8	C_4H_{10}	C_5H_{12}	C_6H_{14}
A01	15.0	1.0		8.59	247.83	7.82	205.7			0.790	0.210									
A02	450.0	1.3		8.59	247.83	7.82	397.5			0.790	0.210									
P01	25.0	1.0	44.0	1.06	97.22	3.07	0.1													
P02	500.0	1.0	29.3	3.76	145.83	4.60	241.1													
P03	850.0	1.0	30.9	5.93	145.84	4.60	553.6	0.036	0.455					0.167	0.189	0.057	0.001			
P04	230.0	1.0	30.9	5.93	145.84	4.60	247.4	0.036	0.455					0.167	0.189	0.057	0.001			
P05	216.6	1.0	32.0	6.02	159.73	5.04	244.3	0.036	0.449					0.165	0.187	0.056	0.001			
P06	43.0	1.0	30.5	5.90	142.06	4.48	90.6	0.036	0.457					0.168	0.190	0.057	0.001			
P07	43.2	1.0	44.2	3.51	100.19	3.16	91.7	0.061	0.074					0.283	0.322	0.099	0.002			
P08	200.4	1.0	43.6	0.11	17.67	0.56	0.03													
P09	200.4	1.0	43.6	0.02	3.78	0.12	0.01													
P10	35.0	31.4	47.5	3.03	78.20	2.47	2.06	0.071						0.327	0.371	0.111	0.002			
P11	−45.0	31.4	47.5	3.03	78.20	2.47	0.71	0.071						0.327	0.371	0.111	0.002			
P12	5.0	26.0	46.4	1.81	61.56	1.94	0.39								0.615	0.185	0.004	0.002		
P13	70.0	16.0	45.2	0.54	25.69	0.81	0.50									0.592	0.013	0.005		0.002
P14	50.0	3.0	44.4	0.18	10.28	0.32	1.15									0.087	0.003	0.012		0.005
P15	−16.8	25.0	47.2	1.27	35.87	1.13	0.74								0.878	0.012				
P16	−17.1	18.0	47.2	1.27	36.00	1.14	1.18								0.895	0.012				
P17	**15.0**	**18.0**	**47.2**	**1.14**	**31.86**	**1.00**	**1.31**								**0.999**					
P18	25.0	1.0	51.7	0.42	5.73	0.18	10.37					0.002		0.814	0.007					
P19	−7.5	18.0	47.3	0.13	4.14	0.13	0.01								0.003	0.111				
P20	40.5	14.0	45.8	0.36	15.41	0.49	0.52									0.847	0.018	0.002		
P21	68.0	21.0	45.8	0.36	15.49	0.49	0.36									0.883	0.054	0.002		
P22	41.4	17.0	45.8	0.31	13.01	0.41	0.35									0.994	0.006			
P23	65.2	17.0	45.7	0.05	2.48	0.08	0.01									0.208	0.351	0.013		
P24	30.3	2.7	45.5	0.15	8.04	0.25	1.34									0.104	0.004	0.015		
P25	95.6	2.0	40.7	0.21	17.48	0.55	0.04									0.003				0.009
P26	95.5	2.0	40.7	0.18	15.24	0.48	0.02									0.004				0.006
S01	296.1	100.0		8.33	150.00	4.73	3.71		1.0											
S02	178.8	7.0		0.64	11.50	0.36	3.30		1.0											
S03	230	7.0		2.70	48.61	1.52	15.7		1.0											
U01	257.8	1.0	47.6	1.13	20.38	0.64	30.71	0.065				0.001		0.301	0.003	0.036	0.016	0.003		
U02	25.0	1.0	51.7	0.80	10.91	0.34	19.76	0.177				0.002		0.814	0.007					
H2-1	50.0	20.0	120.0	0.06	0.13	0.004	0.09	1.000												
H2-2	75.0	14.0	120.0	0.04	0.08	0.003	0.08	1.000												
EX01	172.5	1.0		9.32	258.75	8.16	345.1		0.156	0.728	0.045		0.071							

Table 12
Mass balance of the naphtha steam cracking plant shown in Fig. 1 – part B.

#stream	Composition mol.															
	C_7H_{16}	C_8H_{18}	C_9H_{20}	C_6H_6	C_7H_8	C_8H_{10}-EB	C_8H_{10}-X	C_8H_8	C_2H_2	C_2H_6	C_3H_4-MA	$C_3H_4=$	$C_4H_4=$	$C_4H_6=$	$C_4H_8=$	$C_{12}H_{26}$	C_9H_{12}
A01																	
A02																	
P01																	
P02																	
P03				0.020	0.006	0.001	0.002	0.002	0.007	0.016	0.006		0.001	0.016	0.010	0.003	0.001
P04				0.020	0.006	0.001	0.002	0.002	0.007	0.016	0.006		0.001	0.016	0.010	0.003	0.001
P05				0.020	0.006	0.001	0.002	0.002	0.007	0.016	0.006			0.016	0.009	0.015	0.004
P06				0.020	0.006	0.001	0.002	0.002	0.007	0.016	0.006		0.001	0.016	0.010		
P07				0.036	0.011	0.002	0.004	0.003	0.012	0.028	0.011		0.002	0.030	0.017		
P08																0.792	0.207
P09																0.792	0.207
P10				0.008					0.014	0.032	0.012		0.002	0.029	0.018		
P11				0.008					0.014	0.032	0.012		0.002	0.029	0.018		
P12				0.014					0.023	0.054	0.020		0.003	0.049	0.030		
P13				0.046	0.002						0.066		0.010	0.163	0.102		
P14				0.138	0.005						0.051		0.026	0.474	0.199		
P15									0.034	0.077							
P16										0.093							
P17										**0.001**							
P18																	
P19										0.886							
P20											0.073		0.002	0.005	0.052		
P21													0.002	0.005	0.052		
P22																	
P23													0.016	0.038	0.372		
P24											0.060		0.031	0.550	0.237		
P25			0.012	0.578	0.176	0.030	0.066	0.053			0.002		0.002	0.051	0.008		0.009
P26			0.014	0.531	0.199	0.035	0.077	0.061			0.002		0.002	0.048	0.009		0.010
S01																	
S02																	
S03																	
U01										0.103	0.008		0.005	0.076	0.049		
U02																	
H2-1																	
H2-2																	
EX01																	

A.4. Oxidative coupling of methane plant **Case#3-ref** (refer to Fig. 2)

Table 13

Table 13
Mass balance of the OCM plant depicted in Fig. 2..

#stream	T	p	LHV	Flowrate				Composition, mol.									
	°C	bar	MJ/kg	kmol/s	kg/s	MTPY	m^3/s	O_2	N_2	AR	CH_4	C_2H_4	C_2H_6	CO	H_2	CO_2	H_2O
A01	25.0	1.01	0.0	21.11	609.13	19.21	523.10	0.208	0.783	0.010							
A02	25.0	1.01	0.0	16.50	460.82	14.53	395.74	0.000	0.996	0.004							
A03	25.0	25	0.0	4.61	148.30	4.68	4.47	0.950	0.019	0.031							
A04	25.0	1.01	0.0	10.16	293.02	9.24	251.64	0.208	0.783	0.010							
EX01	152.9	1.01	0.0	11.68	324.67	10.24	413.57	0.017	0.707	0.012						0.085	0.179
P01	25.0	70	46.0	4.93	85.00	2.68	1.50		0.030		0.920		0.040			0.010	
P02	280.0	70	46.0	4.93	85.00	2.68	3.24		0.030		0.920		0.040			0.010	
P03	365.7	11.9	29.7	19.07	374.88	11.82	85.21		0.119	0.067	0.689	0.001	0.018	0.001	0.025	0.019	0.061
P04	600.0	9	15.8	65.65	1253.49	39.53	530.01		0.072	0.044	0.242	0.036	0.005	0.061	0.156	0.052	0.332
P05	600.0	9	15.8	23.53	449.27	14.17	189.96		0.072	0.044	0.242	0.036	0.005	0.061	0.156	0.052	0.332
P06	305.0	9	15.8	23.53	449.27	14.17	125.28		0.072	0.044	0.242	0.036	0.005	0.061	0.156	0.052	0.332
P07	183.0	9	15.8	42.12	804.22	25.36	175.83		0.072	0.044	0.242	0.036	0.005	0.061	0.156	0.052	0.332
P08	40.0	9	22.9	21.98	431.21	13.60	63.11		0.107	0.065	0.360	0.053	0.007	0.091	0.232	0.077	0.007
P09	51.6	10.1	22.9	22.19	435.30	13.73	58.90		0.107	0.065	0.360	0.053	0.007	0.091	0.232	0.077	0.007
P10	40.0	9	27.9	20.12	353.70	11.15	57.91		0.117	0.071	0.393	0.058	0.008	0.099	0.254		
P11	−95.0	34	27.9	20.12	353.70	11.15	7.21		0.117	0.071	0.393	0.058	0.008	0.099	0.254		
P12	−30.6	18	47.2	1.32	37.27	1.18	0.33					0.883	0.117				
P13	−32.6	18	47.1	1.15	32.17	1.01	0.95					0.995	0.005				
P14	15.0	18	47.1	1.15	32.17	1.01	1.32					0.995	0.005				
P15	−15.2	18	47.5	0.17	5.10	0.16	0.01					0.135	0.865				
P16	35.0	13	25.7	18.81	316.43	9.98	36.86		0.125	0.076	0.421			0.106	0.272		
P17	35.0	13	25.7	16.93	284.79	8.98	33.17		0.125	0.076	0.421			0.106	0.272		
P18	409.7	13	24.6	13.97	284.79	8.98	66.75		0.152	0.092	0.616			0.0001	0.033	0.022	0.083
P19	350.0	10.5	0.0	16.37	295	9.24	79.14										1.0
P20	38.0	110	25.7	1.88	31.64	0.99	3.69		0.125	0.076	0.421			0.106	0.272		
W01	305.0	105		9.82	176.92	5.58	0.28										1.0
W02	315.0	100		9.82	176.92	5.58	3.42										1.0
W03	305.0	105		11.72	211.06	6.66	0.33										1.0
W04	500.0	92		11.72	211.06	6.66	7.48										1.0
W05	305.0	105		4.29	77.20	2.43	0.12										1.0
W06	315.0	100		4.29	77.20	2.43	1.49										1.0
W07	140.0	120		3.23	58.11	1.83	0.07										1.0
W08	315.0	100		17.33	312.23	9.85	6.04										1.0
W09	500.0	92		29.05	523.29	16.50	18.56										1.0
W10	171.1	6		1.84	33.08	1.04	10.93										1.0
W11	44.5	0.08		27.21	490.21	15.46	7752.00										1.0

References

[1] Alstom Power Energy Recovery. Gas cooling systems for steam reforming plants; n.d.
[2] Lippe D. Ethylene production bounces back; turnarounds in early 2013 to curb output. Oil Gas J 2012;2013:111.
[3] IEA. Tracking industrial energy efficiency and CO_2 emissions energy; 2007.
[4] European Commission. Reference document on best available techniques in the large volume organic chemical industry - chapter 7; 2003.
[5] Chen JQ, Bozzano A, Glover B, Fuglerud T, Kvisle S. Recent advancements in ethylene and propylene production using the UOP/Hydro MTO process. Catal Today 2005;106:103–7. http://dx.doi.org/10.1016/j.cattod.2005.07.178.
[6] Xiang D, Qian Y, Man Y, Yang S. Techno-economic analysis of the coal-to-olefins process in comparison with the oil-to-olefins process. Appl Energy 2014;113:639–47. http://dx.doi.org/10.1016/j.apenergy.2013.08.013.
[7] EU-OPEC Energy Dialogues. Petrochemical Outlook - Challenges and Opportunities. 2014.
[8] Boulamanti A, Moya JA. Production costs of the chemical industry in the EU and other countries: ammonia, methanol and light olefins. Renew Sustain Energy Rev 2017;68:1205–12. http://dx.doi.org/10.1016/j.rser.2016.02.021.
[9] Ren T, Patel MK, Blok K. Steam cracking and methane to olefins: energy use, CO_2 emissions and production costs. Energy 2008;33:817–33. http://dx.doi.org/10.1016/j.energy.2008.01.002.
[10] Xiang D, Yang S, Li X, Qian Y. Life cycle assessment of energy consumption and GHG emissions of olefins production from alternative resources in China. Energy Convers Manag 2015;90:12–20. http://dx.doi.org/10.1016/j.enconman.2014.11.007.
[11] Benchaita T. Greenhouse gas emissions from new petrochemical plants; 2013.
[12] Gradassi MJ, Green NW. Economics of natural gas conversion processes. Fuel Process Technol 1995;42:65–83. http://dx.doi.org/10.1016/0378-3820(94)00094-A.
[13] Godini HR, Gili A, Görke O, Simon U, Hou K, Wozny G. Performance analysis of a porous packed bed membrane reactor for oxidative coupling of methane: structural and operational characteristics. Energy Fuels 2014;28:877–90. http://dx.doi.org/10.1021/ef402041b.
[14] Deboy JM, Hicks RF. Kinetics of the oxidative coupling of methane over 1 wt% Sr La_2O_3. J Catal 1988;113:517–24. http://dx.doi.org/10.1016/0021-9517(88)90277-1.
[15] Mleczko L, Baerns M. Catalytic oxidative coupling of methane - reaction engineering aspects and process schemes. Fuel Process Technol 1995;42:217–48.
[16] Stansch Z, Mleczko L, Baerns M. Comprehensive kinetics of oxidative coupling of methane over the La_2O_3/CaO catalyst. Ind Eng Chem Res 1997;36:2568–79. http://dx.doi.org/10.1021/ie960562k.
[17] Keller GE, Bhasin MM. Synthesis of ethylene via oxidative coupling of methane I. Determination of active catalysts. J Catal 1982;73:9–19. http://dx.doi.org/10.1016/0021-9517(82)90075-6.
[18] Otsuka K, Jinno K, Morikawa A. Active and selective catalysts for the synthesis of C_2H_4 and C_2H_6 via oxidative coupling of methane. J Catal 1986;100:353–9. http://dx.doi.org/10.1016/0021-9517(86)90102-8.
[19] Otsuka K, Hatano M, Komatsu T. Synthesis of C_2H_4 by partial oxidation of CH_4 over transition metal oxides with alkali-chlorides. In: Bibby DM, Howe RF, Yurchak S, BT - Studies in Surface Science and Catalysis CDC, editors. Methane Convers. Proc. a Symp. Prod. Fuels Chem. from Nat. Gas, vol. 36, Elsevier; 1988, p. 383–7. doi:http://dx.doi.org/10.1016/S0167-2991(09)60529-2.
[20] Ito T, Wang J, Lin CH, Lunsford JH. Oxidative dimerization of methane over a

lithium-promoted magnesium oxide catalyst. J Am Chem Soc 1985;107:5062–8. http://dx.doi.org/10.1021/ja00304a008.
[21] Korf SJ, Roos JA, De Bruijn NA, Van Ommen JG, Ross JRH. Lithium chemistry of lithium doped magnesium oxide catalysts used in the oxidative coupling of methane. Appl Catal 1990;58:131–46.
[22] Sofranko JA, Leonard JJ, Jones CA. The oxidative conversion of methane to higher hydrocarbons. J Catal 1987;103:302–10.
[23] Wu J, Li S. The role of distorted WO_4 in the oxidative coupling of methane on supported tungsten oxide catalysts. J Phys Chem 1995;99:4566–8. http://dx.doi.org/10.1021/j100013a030.
[24] Pak S, Qiu P, Lunsford JH. Elementary reactions in the oxidative coupling of methane over $Mn/Na_2WO_4/SiO_2$ and $Mn/Na_2WO_4/MgO$ catalysts. J Catal 1998;179:222–30.
[25] Vatani A, Jabbari E, Askarieh M, Torangi MA. Kinetic modeling of oxidative coupling of methane over Li/MgO catalyst by genetic algorithm. J Nat Gas Sci Eng 2014;20:347–56. http://dx.doi.org/10.1016/j.jngse.2014.07.005.
[26] Liu H, Wang X, Yang D, Gao R, Wang Z. Scale up and stability test for oxidative coupling of methane over Na_2WO_4 -Mn/SiO_2 catalyst in a 200 ml fixed-bed reactor. Nat Gas Chem 2008;17:59–63.
[27] Lee JY, Jeon W, Choi JW, Suh YW, Ha JM, Suh DJ, et al. Scaled-up production of C_2 hydrocarbons by the oxidative coupling of methane over pelletized $Na_2WO_4/Mn/SiO_2$ catalysts: observing hot spots for the selective process. Fuel 2013;106:851–7. http://dx.doi.org/10.1016/j.fuel.2013.01.026.
[28] Tiemersma TP, Chaudhari AS, Gallucci F, Kuipers JAM, van Sint Annaland M. Integrated autothermal oxidative coupling and steam reforming of methane. Part 2: development of a packed bed membrane reactor with a dual function catalyst. Chem Eng Sci 2012;82:232–45. http://dx.doi.org/10.1016/j.ces.2012.07.047.
[29] Tiemersma TP, Chaudhari AS, Gallucci F, Kuipers JAM, van Sint Annaland M. Integrated autothermal oxidative coupling and steam reforming of methane. Part 1: design of a dual-function catalyst particle. Chem Eng Sci 2012;82:200–14. http://dx.doi.org/10.1016/j.ces.2012.07.048.
[30] Tiemersma TP, Kolkman T, Kuipers JAM, van Sint Annaland M. A novel autothermal reactor concept for thermal coupling of the exothermic oxidative coupling and endothermic steam reforming of methane. Chem Eng J 2012;203:223–30. http://dx.doi.org/10.1016/j.cej.2012.07.021.
[31] Jašo S, Godini HR, Arellano-Garcia H, Omidkhah M, Wozny G. Analysis of attainable reactor performance for the oxidative methane coupling process. Chem Eng Sci 2010;65:6341–52. http://dx.doi.org/10.1016/j.ces.2010.08.019.
[32] Nouralishahi A, Pahlavanzadeh H, Towfighi Daryan J. Determination of optimal temperature profile in an OCM plug flow reactor for the maximizing of ethylene production. Fuel Process Technol 2008;89:667–77. http://dx.doi.org/10.1016/j.fuproc.2007.12.004.
[33] Sadjadi S, Simon U, Godini HR, Görke O, Schomäcker R, Wozny G. Reactor material and gas dilution effects on the performance of miniplant-scale fluidized-bed reactors for oxidative coupling of methane. Chem Eng J 2015;281:678–87. http://dx.doi.org/10.1016/j.cej.2015.06.079.
[34] Godini HR, Xiao S, Jašo S, Stünkel S, Salerno D, Son NX, et al. Techno-economic analysis of integrating the methane oxidative coupling and methane reforming processes. Fuel Process Technol 2013;106:684–94. http://dx.doi.org/10.1016/j.fuproc.2012.10.002.
[35] Bhatia S, Thien CY, Mohamed AR. Oxidative coupling of methane (OCM) in a catalytic membrane reactor and comparison of its performance with other catalytic reactors. Chem Eng J 2009;148:525–32. http://dx.doi.org/10.1016/j.cej.2009.01.008.
[36] Godini HR, Xiao S, Kim M, Gorke O, Song S, Wozny G. Dual-membrane reactor for methane oxidative coupling and dry methane reforming: reactor integration and process intensification. Chem Eng Process Process Intensif 2013;74:153–64. http://dx.doi.org/10.1016/j.cep.2013.09.007.
[37] Kao YK, Lei L, Lin YS. Optimum operation of oxidative coupling of methane in porous ceramic membrane reactors. Catal Today 2003;82:255–73. http://dx.doi.org/10.1016/S0920-5861(03)00240-2.
[38] Cruellas Labella A, Melchiori T, Gallucci F, Van Sint Annaland M. Advanced reactor concepts for oxidative coupling of methane. Catal Rev 2017;59(03):234–94. http://dx.doi.org/10.1080/01614940.2017.1348085.
[39] Thiruvenkataswamy P, Eljack FT, Roy N, Mannan MS, El-Halwagi MM. Safety and techno-economic analysis of ethylene technologies. J Loss Prev Process Ind 2016;39:74–84. http://dx.doi.org/10.1016/j.jlp.2015.11.019.
[40] Khojasteh Salkuyeh Y, Adams TA. A novel polygeneration process to co-produce ethylene and electricity from shale gas with zero CO_2 emissions via methane oxidative coupling. Energy Convers Manag 2015;92:406–20. http://dx.doi.org/10.1016/j.enconman.2014.12.081.
[41] Stünkel S, Illmer D, Drescher A, Schomäcker R, Wozny G. On the design, development and operation of an energy efficient CO_2 removal for the oxidative coupling of methane in a miniplant scale. Appl Therm Eng 2012;43:141–7. http://dx.doi.org/10.1016/j.applthermaleng.2011.10.035.
[42] Zimmermann H, Walzl R. Ethylene. Ullmann's Encycl Ind Chem 2012:547–72. http://dx.doi.org/10.1002/14356007.a10.
[43] EBTF. European best practice guidelines for assessment of CO_2 capture technologies; 2011.
[44] Hassan Al-Haj I. Design of fractionation columns, MATLAB applications for the practical engineer 2014, doi:10.5772/57249.
[45] Beysel G. Enhanced cryogenic air separation a proven process applied to oxyfuel: future prospects. In: 1st Oxyfuel combustion conference; 2009.
[46] Crotti G. Analisi di unitá criogeniche per il frazionamento dell'aria. Politecnico di Milano; 2010.
[47] Jones D, Bhattacharyya D, Turton R, Zitney SE. Optimal design and integration of an air separation unit (ASU) for an integrated gasification combined cycle (IGCC) power plant with CO_2 capture. Fuel Process Technol 2011;92:1685–95. http://dx.doi.org/10.1016/j.fuproc.2011.04.018.
[48] Smith AR, Klosek J. A review of air separation technologies and their integration with energy conversion processes. Fuel Process Technol 2001;70:115–34. http://dx.doi.org/10.1016/S0378-3820(01)00131-X.
[49] The Linde Group. Tonnage air separation plants; n.d.
[50] Manzolini G, Macchi E, Gazzani M. CO_2 capture in natural gas combined cycle with SEWGS. Part B: economic assessment. Int J Greenh Gas, Control 2013;12:502–9. http://dx.doi.org/10.1016/j.ijggc.2012.06.021.
[51] Spallina V, Pandolfo D, Battistella A, Romano MC, Van Sint Annaland M, Gallucci F. Techno-economic assessment of membrane assisted fluidized bed reactors for pure H2 production with CO_2 capture. Energy Convers Manag 2016;120:257–73. http://dx.doi.org/10.1016/j.enconman.2016.04.073.
[52] Fini T, Patz C, Wentzel R. Oxidative coupling of methane to ethane. University of Pennsylvania; 2014, doi:10.1016/S0166-9834(00)81610-3.
[53] Dutch Association of Cost Engineers. Price Booklet edition nr. 30. 30th ed. Michael Sprong; 2014.
[54] d'Accadia MD, de Rossi F. Thermoeconomic optimization of a refrigeration plant. Int J Refrig 1998;21:42–54. http://dx.doi.org/10.1016/S0140-7007(97)00071-6.
[55] Hoebink JHBJ, Venderboesch HM, van Geem PC, Marin GB. Economics of the oxidative coupling of methane as an add-on unit for naphtha cracking. Chem Eng Technol 1995;18:12–6.
[56] Fábrega FM, Rossi JS, D'Angelo JVH. Exergoeconomic analysis applied in the optimization of refrigeration system in ethylene and propylene production process. In: 10th Symposium on Process System Engineering - PSE2009, vol. 27; 2009. p. 549–54, doi:http://dx.doi.org/10.1016/S1570-7946(09)70312-8.
[57] Gazzani M, Turi DM, Manzolini G. Techno-economic assessment of hydrogen selective membranes for CO2 capture in integrated gasification combined cycle. Int J Greenh Gas Control 2014;20:293–309. http://dx.doi.org/10.1016/j.ijggc.2013.11.006.
[58] DOE/NETL. Cost and performance baseline for fossil energy plants, Coal to synthetic natural gas and ammonia, vol. 2; 2011. doi:DOE/NETL-2010/1402.
[59] Cleaver Brooks. Boiler efficiency guide 2010:22.
[60] Iea - Energy Technology Group. Industrial Combustion Boilers 2010:1–5, doi:http://dx.doi.org/10.1201/EBK1420085280.
[61] DOE/NETL. Assessment of hydrogen production with CO_2 capture, Baseline State-of- the-Art Plants, vol. 1; 2010.
[62] Rubin ES, Davison JE, Herzog HJ. The cost of CO_2 capture and storage. Int J Greenh Gas Control 2015;40:378–400. http://dx.doi.org/10.1016/j.ijggc.2015.05.018.
[63] Manzolini G, Dijkstra JW, Macchi E, Jansen D. Technical Economic Evaluation of a system for electricity production CO_2 capture using membrane reformer with permeate side combustion. In: ASME Turbo Expo 2006, Barcelona; 2006. p. 1–11.
[64] Haghighi SS, Rahimpour MR, Raeissi S, Dehghani O. Investigation of ethylene production in naphtha thermal cracking plant in presence of steam and carbon dioxide. Chem Eng J 2013;228:1158–67. http://dx.doi.org/10.1016/j.cej.2013.05.048.
[65] Dautzenberg FM, Schlatter JC, Fox JM, Rostrup-Nielsen JR, Christiansen LJ. Catalyst and reactor requirements for the oxidative coupling of methane. Catal Today 1992;13:503–9.
[66] Baasel WD. Preliminary chemical engineering plant design. New York: Van Nostrand Reinhold; 1989.
[67] Gerdes K, Summers WM, Wimer J. Cost Estimation Methodology for NETL assessments of power plant performance. Pittsburgh; 2011.